

CHAPTER
ONE

Basic Ideas About Turbulence

1.1 THE FUNDAMENTAL PROBLEM OF TURBULENCE

1.1.1 The Closure Problem

$$\frac{du}{dt} + uu + ru = 0 \quad (1.1)$$

$$\frac{d\bar{u}}{dt} + \bar{u}\bar{u} + r\bar{u} = 0 \quad (1.2)$$

$$\overline{uu} = \bar{u}\bar{u} + \overline{u'u'} \neq \bar{u}\bar{u} \quad (1.3)$$

$$\frac{1}{2} \frac{d\bar{u}^2}{dt} + \overline{uuu} + r\bar{u}^2 = 0 \quad (1.4)$$

Suppose that:

$$\overline{uuuu} = \alpha \bar{u}\bar{u}\bar{u}\bar{u} + \beta \overline{uuuu} \quad (1.5)$$

where α and β are some parameters, and closures set in physical space or in spectral space.

Navier-Stokes equations:

$$\frac{\partial \bar{u}}{\partial t} + (\bar{\mathbf{v}} \cdot \nabla) \bar{u} = -\frac{\partial \bar{p}}{\partial x} - \nabla \cdot \overline{\mathbf{v}'u'}. \quad (1.6)$$

In Cartesian coordinates

$$\nabla \cdot \overline{\mathbf{v}'u'} = \frac{\partial}{\partial x} \overline{u'u'} + \frac{\partial}{\partial y} \overline{u'v'} + \frac{\partial}{\partial z} \overline{u'w'} \quad (1.7)$$

These are *Reynolds stress* terms.

1.1.2 Triad Interactions

$$\frac{D\zeta}{Dt} = \frac{\partial \zeta}{\partial t} + J(\psi, \zeta) = F + \nu \nabla^2 \psi, \quad \zeta = \nabla^2 \psi. \quad (1.8)$$

$$\psi(x, y, t) = \sum_{\mathbf{k}} \tilde{\psi}(\mathbf{k}, t) e^{i\mathbf{k}\cdot\mathbf{x}}, \quad \zeta(x, y, t) = \sum_{\mathbf{k}} \tilde{\zeta}(\mathbf{k}, t) e^{i\mathbf{k}\cdot\mathbf{x}}, \quad (1.9)$$

where $\mathbf{k} = \mathbf{i}k^x + \mathbf{j}k^y$, $\tilde{\zeta} = -k^2 \tilde{\psi}$
 $k^2 = k^{x^2} + k^{y^2}$
 $\tilde{\psi}(k^x, k^y, t) = \tilde{\psi}^*(-k^x, -k^y, t)$,

$$\begin{aligned} \frac{\partial}{\partial t} \sum_{\mathbf{k}} \tilde{\zeta}(\mathbf{k}, t) e^{i\mathbf{k}\cdot\mathbf{x}} = & - \sum_{\mathbf{p}} p^x \tilde{\psi}(\mathbf{p}, t) e^{i\mathbf{p}\cdot\mathbf{x}} \times \sum_{\mathbf{q}} q^y \tilde{\zeta}(\mathbf{q}, t) e^{i\mathbf{q}\cdot\mathbf{x}} \\ & + \sum_{\mathbf{p}} p^y \tilde{\psi}(\mathbf{p}, t) e^{i\mathbf{p}\cdot\mathbf{x}} \times \sum_{\mathbf{q}} q^x \tilde{\zeta}(\mathbf{q}, t) e^{i\mathbf{q}\cdot\mathbf{x}}. \end{aligned} \quad (1.10)$$

Multiply (1.10) by $\exp(-i\mathbf{k}\cdot\mathbf{x})$ and integrating over the domain,

$$\int e^{i\mathbf{p}\cdot\mathbf{x}} e^{i\mathbf{q}\cdot\mathbf{x}} dA = \frac{1}{L^2} \delta(\mathbf{p} + \mathbf{q}). \quad (1.11)$$

Using this, (1.10) becomes

$$\frac{\partial}{\partial t} \tilde{\psi}(\mathbf{k}, t) = \sum_{\mathbf{p}, \mathbf{q}} A(\mathbf{k}, \mathbf{p}, \mathbf{q}) \tilde{\psi}(\mathbf{p}, t) \tilde{\psi}(\mathbf{q}, t) + \tilde{F}(\mathbf{k}) - \nu k^4 \tilde{\psi}(\mathbf{k}, t), \quad (1.12)$$

where $A(\mathbf{k}, \mathbf{p}, \mathbf{q}) = (q^2/k^2)(p^x q^y - p^y q^x) \delta(\mathbf{p} + \mathbf{q} - \mathbf{k})$ (An 'interaction coefficient')

Only triads with $\mathbf{p} + \mathbf{q} = \mathbf{k}$ make a nonzero contribution.

Two types of interactions:

- (i) Local interactions, in which $k \sim p \sim q$;
- (ii) Nonlocal interactions, in which $k \sim p \gg q$.

Assume local triad interactions dominate.

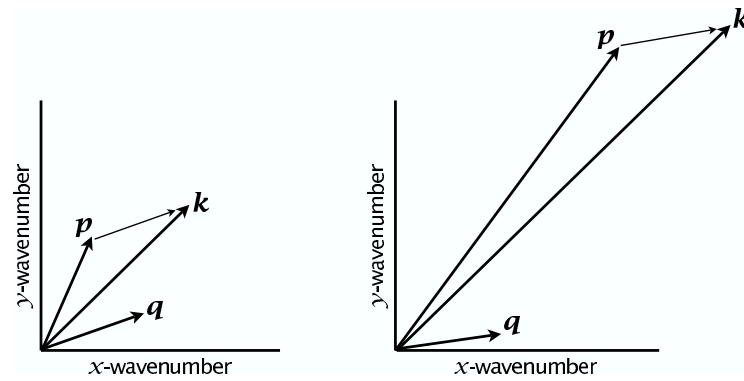


Fig. 1.1 Two interacting triads, each with $k = p + q$. On the left, a local triad with $k \sim p \sim q$. On the right, a nonlocal triad with $k \sim p \gg q$.

1.2 THE KOLMOGOROV THEORY

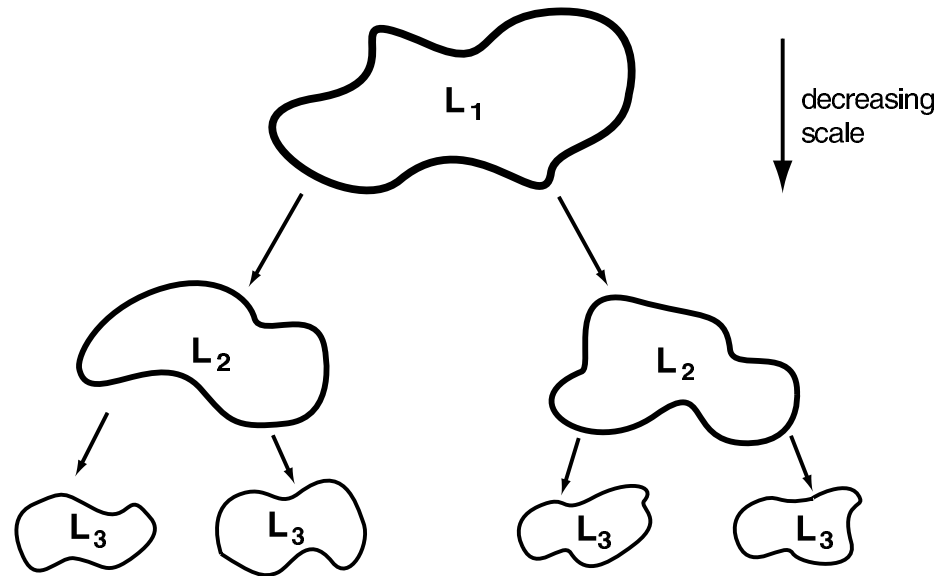


Fig. 1.2 Schema of a transfer of energy to smaller scales.

Consider high Reynolds number (Re) incompressible flow that is being maintained by some external force. Then the evolution of the system is governed by

$$\frac{\partial \mathbf{v}}{\partial t} + (\mathbf{v} \cdot \nabla) \mathbf{v} = -\nabla p + \mathbf{F} + \nu \nabla^2 \mathbf{v} \quad (1.13)$$

and

$$\nabla \cdot \mathbf{v} = 0 \quad (1.14)$$

The energy equation is

$$\frac{d\hat{E}}{dt} = \frac{d}{dt} \int \frac{1}{2} \mathbf{v}^2 dV = \int (\mathbf{F} \cdot \mathbf{v} + \nu \mathbf{v} \cdot \nabla^2 \mathbf{v}) dV = \int (\mathbf{F} \cdot \mathbf{v} - \nu \boldsymbol{\omega}^2) dV \quad (1.15)$$

where \hat{E} is the total energy. Must include viscosity!

Viscous terms will important when

$$L_\nu \sim \frac{\nu}{V}. \quad (1.16)$$

Millimeters! Energy cascades to small scales!

1.2.1 The theory and scaling of Kolmogorov

$$u(x, y, z, t) = \sum_{k^x, k^y, k^z} \tilde{u}(k^x, k^y, k^z, t) e^{i(k^x x + k^y y + k^z z)} \quad (1.17)$$

Energy:

$$\hat{E} = \int E \, dV = \frac{1}{2} \int (u^2 + v^2 + w^2) \, dV = \mathcal{E}(k) \, dk \quad (1.18)$$

where $\mathcal{E}(k)$ is the energy spectral density, or the energy spectrum,

Assume:

- (i) There exists a range of scales intermediate between the large scale and the dissipation scale where neither forcing nor dissipation are explicitly important to the dynamics.
- (ii) There is a constant flux of energy from large scales equal to ε .

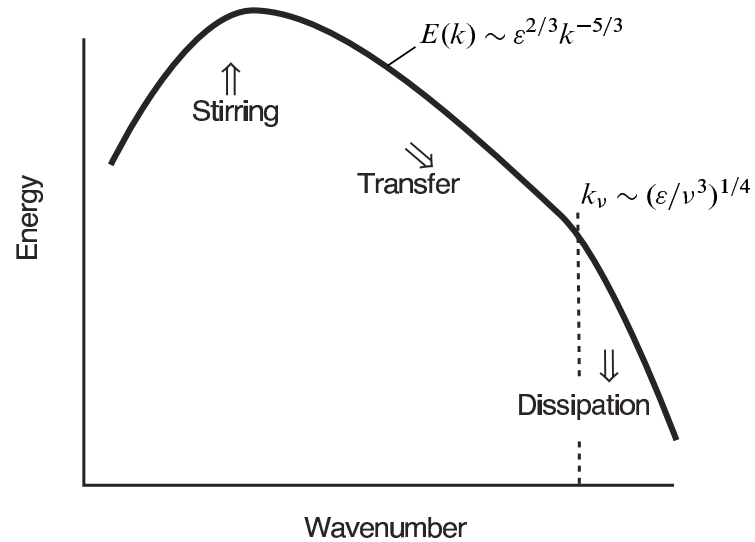
Write:

$$\mathcal{E}(k) = g(\varepsilon, k, k_0, k_\nu) \quad (1.19)$$

In inertial range:

$$\mathcal{E}(k) = g(\varepsilon, k). \quad (1.20)$$

The function g is, within this theory, *universal*, the same for every turbulent flow.

**Quantity**Wavenumber, k Energy per unit mass, E Energy spectrum, $\mathcal{E}(k)$ Energy Flux, ϵ **Dimension**

1/L

 $U^2 = L^2/T^2$ $EL = L^3/T^2$ $E/T = L^2/T^3$

If $\mathcal{E} = f(\epsilon, k)$ then the only dimensionally consistent relation for the energy spectrum is

$$\mathcal{E} = \mathcal{K} \epsilon^{2/3} k^{-5/3}$$

where \mathcal{K} is a universal dimensionless constant ≈ 1.5 .

1.2.2 Eddy turnover time

$$\tau_k = [\mathcal{E}(k)k^3]^{-1/2} \quad (1.21)$$

Then we posit that

$$\varepsilon \sim \frac{\mathcal{E}(k)k}{\tau_k} \quad (1.22)$$

So that

$$\varepsilon \sim \frac{\mathcal{E}(k)k}{[\mathcal{E}(k)k^3]^{-1/2}} = [\mathcal{E}(k)]^{3/2}k^{5/2} \quad (1.23)$$

So that

$$\mathcal{E}(k) = \mathcal{K}\varepsilon^{2/3}k^{-5/3} \quad (1.24)$$

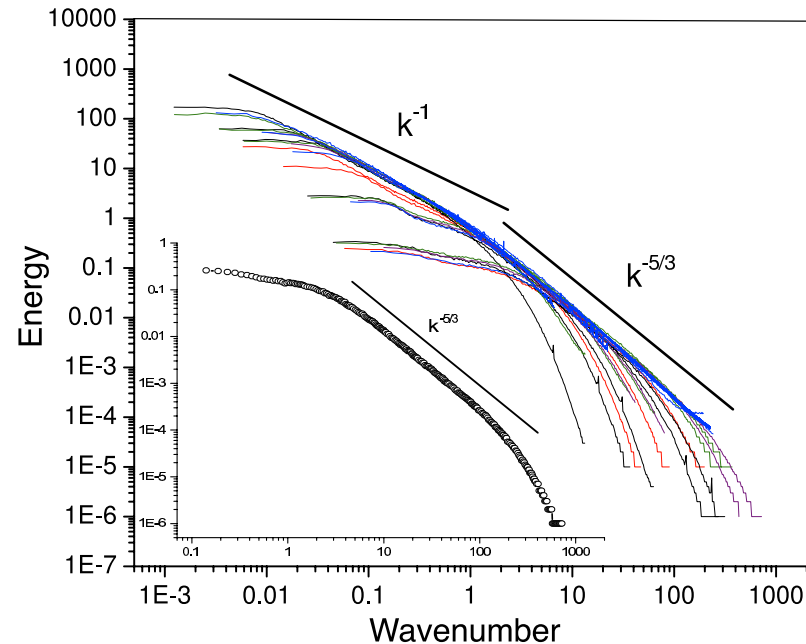


Fig. 1.3 The energy spectrum of 3D turbulence measured in some experiments at the Princeton Superpipe facility. The outer plot shows the spectra from a large-number of experiments at different Reynolds numbers, with the magnitude of their spectra appropriately rescaled. Smaller scales show a good $-5/3$ spectrum, whereas at larger scales the eddies feel the effects of the pipe wall and the spectra are a little shallower. The inner plot shows the spectrum in the centre of the pipe in a single experiment at $Re \approx 10^6$.

The viscous scale and energy dissipation

The viscous term is $\nu \nabla^2 u$ so that a viscous or dissipation timescale at a scale k^{-1} , τ_k^v , is

$$\tau_k^v \sim \frac{1}{k^2 \nu}, \quad (1.25)$$

The eddy turnover time, τ_k — that is, the inertial timescale — in the Kolmogorov spectrum is

$$\tau_k = \varepsilon^{-1/3} k^{-2/3}. \quad (1.26)$$

Give:

$$k_v \sim \left(\frac{\varepsilon}{\nu^3} \right)^{1/4}, \quad L_v \sim \left(\frac{\nu^3}{\varepsilon} \right)^{1/4}. \quad (1.27a,b)$$

L_v is called the *Kolmogorov scale*.

In atmosphere and ocean: $L_v \sim 1 \text{ mm}$.

1.2.3 * An alternative scaling argument for inertial ranges

Euler equations are invariant under

$$x \rightarrow x\lambda \quad v \rightarrow v\lambda^r \quad t \rightarrow t\lambda^{1-r}, \quad (1.28)$$

where r is an arbitrary scaling exponent.

Assume:

- (i) That the flux of energy from large to small scales (i.e., ε) is finite and constant.
- (ii) That the scale invariance (1.28) holds, on a time-average, in the intermediate scales between the forcing scales and dissipation scales.

Dimensional analysis

$$\varepsilon_k \sim \frac{v_k^3}{l_k} \sim \lambda^{3r-1}. \quad (1.29)$$

But ε is independent of scale so $r = 1/3$. The velocity then scales as

$$v_k \sim \varepsilon^{1/3} k^{-1/3}, \quad (1.30)$$

On dimensional grounds,

$$\mathcal{E}(k) \sim v_k^2 k^{-1} \sim \varepsilon^{2/3} k^{-2/3} k^{-1} \sim \varepsilon^{2/3} k^{-5/3}. \quad (1.31)$$

1.3 TWO-DIMENSIONAL TURBULENCE

$$\frac{\partial \zeta}{\partial t} + \mathbf{u} \cdot \nabla \zeta = F + \nu \nabla^2 \zeta \quad (1.32)$$

$u = -\partial\psi/\partial y$, $v = \partial\psi/\partial x$, and $\zeta = \nabla^2\psi$ so that

$$\frac{\partial \nabla^2 \psi}{\partial t} + J(\psi, \nabla^2 \psi) = F + \nu \nabla^4 \psi. \quad (1.33)$$

Two conserved quantities:

$$\hat{E} = \frac{1}{2} \int_A (u^2 + v^2) dA = \frac{1}{2} \int_A (\nabla \psi)^2 dA, \quad \frac{d\hat{E}}{dt} = 0, \quad (1.34a)$$

$$\hat{Z} = \frac{1}{2} \int_A \zeta^2 dA = \frac{1}{2} \int_A (\nabla^2 \psi)^2 dA, \quad \frac{d\hat{Z}}{dt} = 0. \quad (1.34b)$$

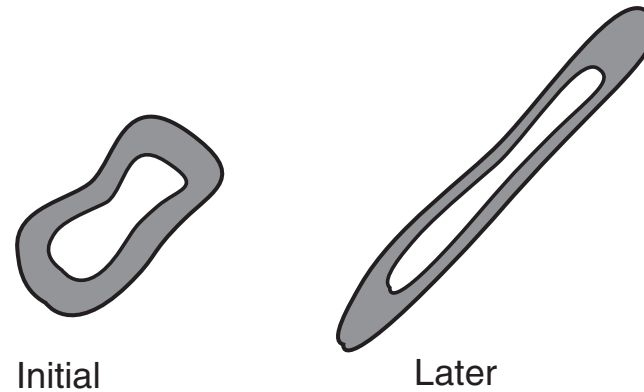


Fig. 1.4 In incompressible two-dimensional flow, a band of fluid will generally be elongated, but its area will be preserved. Since vorticity is tied to fluid parcels, the values of the vorticity in the hatched area (and in the hole in the middle) are maintained; thus, vorticity gradients will increase and the enstrophy is thereby, on average, moved to smaller scales.

1.3.1 Energy and Enstrophy Transfer

Energy is transferred to large scales! Why

Vorticity elongation

Band is elongated. Vorticity gradients increase. Enstrophy moves to small scales

$$\hat{E} = -\frac{1}{2} \int \psi \zeta \, dA, \quad (1.35)$$

Solving the Poisson equation $\nabla^2 \psi = \zeta$ leads to the scale of the streamfunction becoming larger in the direction of stretching, but virtually no smaller in the perpendicular direction. Hence, on average, the scale of the streamfunction increases.

II An energy-ensrophy conservation argument

Total energy and enstrophy:

$$\hat{E} = \int \mathcal{E}(k) dk, \quad \hat{Z} = \int Z(k) dk = \int k^2 \mathcal{E}(k) dk, \quad (1.36)$$

Centroid,

$$k_e = \frac{\int k \mathcal{E}(k) dk}{\int \mathcal{E}(k) dk} \quad (1.37)$$

$$I \equiv \int (k - k_e)^2 \mathcal{E}(k) dk, \quad \frac{dI}{dt} > 0. \quad (1.38)$$

Expanding

$$\begin{aligned} I &= \int k^2 \mathcal{E}(k) dk - 2k_e \int k \mathcal{E}(k) dk + k_e^2 \int \mathcal{E}(k) dk \\ &= \int k^2 \mathcal{E}(k) dk - k_e^2 \int \mathcal{E}(k) dk, \end{aligned} \quad (1.39)$$

because $k_e = \int k \mathcal{E}(k) dk$ is, from (1.37), the energy-weighted centroid.

Because both energy and enstrophy are conserved, (1.39) gives

$$\frac{dk_e^2}{dt} = -\frac{1}{\hat{E}} \frac{dI}{dt} < 0. \quad (1.40)$$

Thus, the centroid of the distribution moves to smaller wavenumber and to larger scale

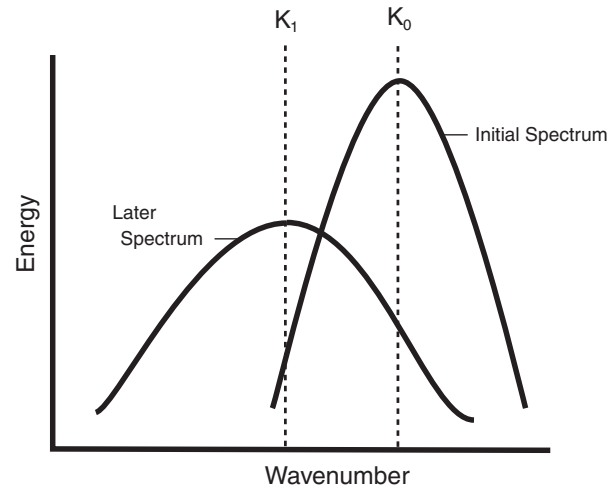


Fig. 1.5 In two-dimensional flow, the centroid of the energy spectrum will move to large scales (smaller wavenumber) provided that the width of the distribution increases, which can be expected in a nonlinear, eddying flow

Enstrophy: Let $j = 1/k$.

$$J = \int (q - q_e)^2 Z(q) dq, \quad \frac{dJ}{dt} > 0, \quad (1.41)$$

But $\int q^2 Z(q) dq$ is conserved - Energy

1.3.2 Enstrophy inertial ranges in 2D turbulence

In the enstrophy inertial range the enstrophy cascade rate η , equal to the rate at which enstrophy is supplied by stirring, is assumed constant. By analogy with (1.22) we may assume that this rate is given by

$$\eta \sim \frac{k^3 \mathcal{E}(k)}{\tau_k}. \quad (1.42)$$

$$\tau_k = [\mathcal{E}(k)k^3]^{-1/2} \quad (1.43)$$

we obtain

$$\boxed{\mathcal{E}(k) = \mathcal{K}_\eta \eta^{2/3} k^{-3}}, \quad (1.44)$$

where \mathcal{K}_η is a universal constant

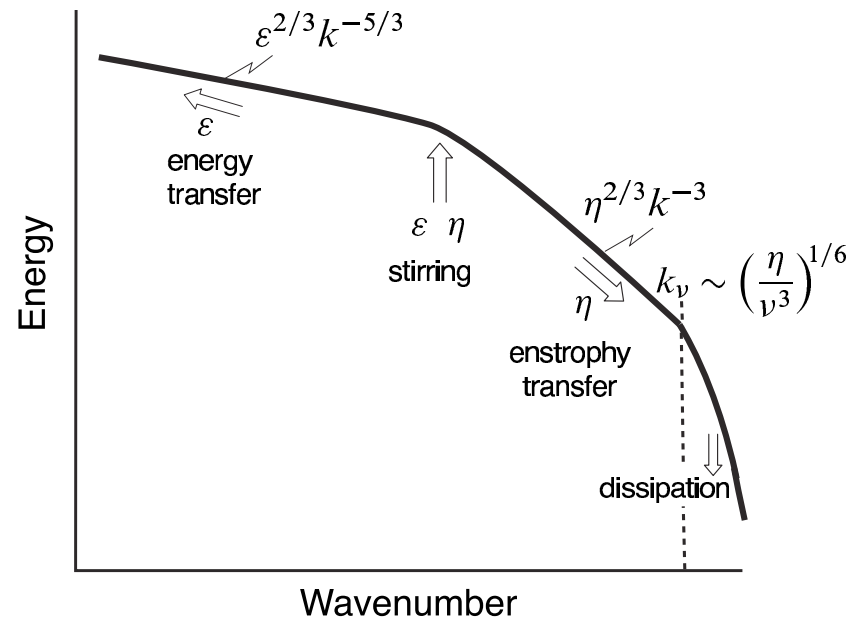


Fig. 1.6 The energy spectrum of two-dimensional turbulence. (Compare with Fig. 1.2.1.) Energy supplied at some rate ε is transferred to large scales, whereas enstrophy supplied at some rate η is transferred to small scales, where it may be dissipated by viscosity. If the forcing is localized at a scale k_f^{-1} then $\eta \approx k_f^2 \varepsilon$.

Energy inertial range

Same as the three-dimensional case,

$$\mathcal{E}(k) = \mathcal{K}_\varepsilon \varepsilon^{2/3} k^{-5/3}, \quad (1.45)$$

Same as 3D case, except energy transfer to *larger* scales.

Equate frictional timescale r^{-1} to inertial timescale:

$$r^{-1} = \varepsilon^{-1/3} k_r^{-2/3} \quad \longrightarrow \quad k_r = \left(\frac{r^3}{\varepsilon} \right)^{1/2}, \quad (1.46)$$

where k_r is the frictional wavenumber. Frictional effects are important at scales *larger* than k_r^{-1} .

1.3.3 Numerical illustrations

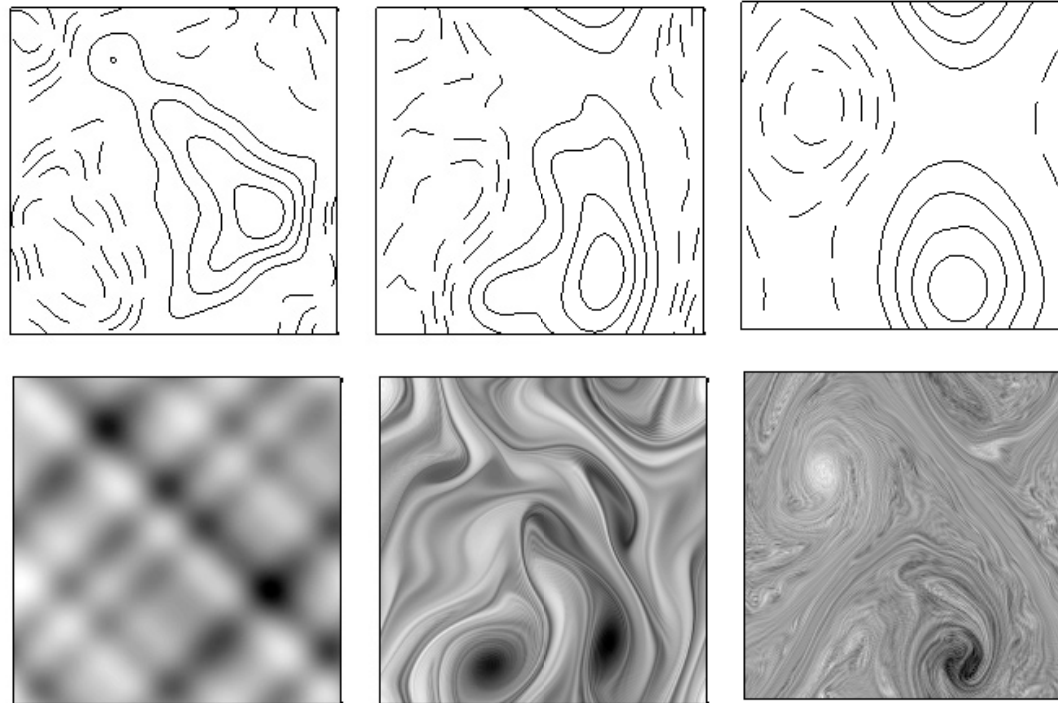


Fig. 1.7 Nearly-free evolution of vorticity (grayscale) and streamfunction (contours).

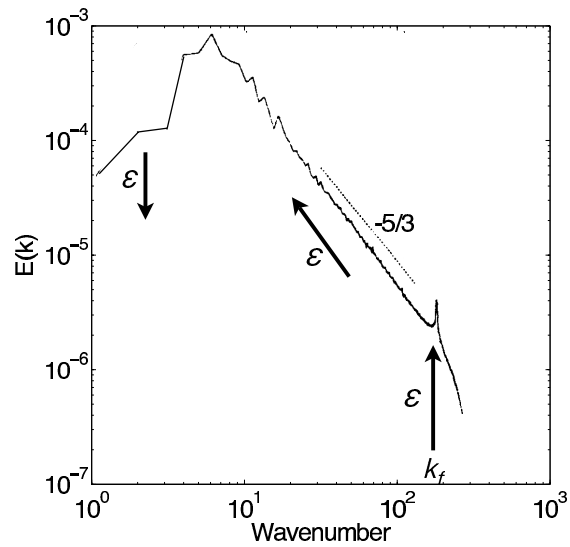


Figure 1.9 The energy spectrum in a numerical simulation of forced-dissipative two-dimensional turbulence. The fluid is stirred at wavenumber k_f and dissipated at large scales with a linear drag, and there is an $k^{-5/3}$ spectrum at intermediate scales. The arrows schematically indicate the direction of the energy flow.

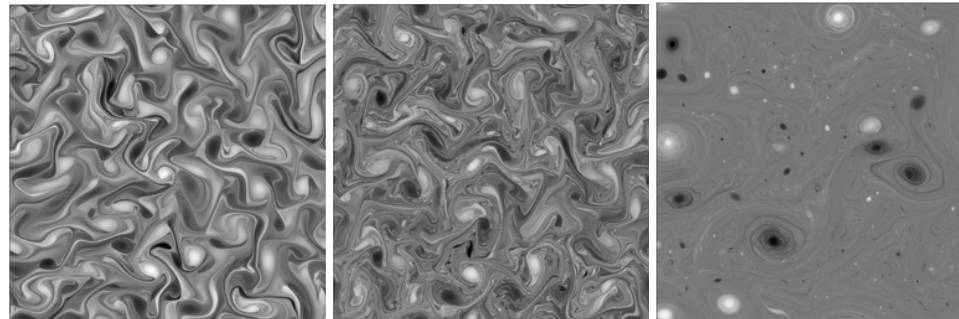


Fig. 1.8 Vorticity evolution

1.4 * PREDICTABILITY OF TURBULENCE

Weather is unpredictable! Why? How much?

Errors cascade to larger scales.

Time taken is:

$$T = \int_{k_0}^{k_1} \tau_k d(\ln k) = \int_{k_0}^{k_1} [k^3 \mathcal{E}(k)]^{-1/2} d(\ln k), \quad (1.47)$$

treating the wavenumber spectrum as continuous.

If $E = Ak^{-n}$ we get:

$$T = \frac{2}{A^{1/2}(n-3)} \left[k^{(n-3)/2} \right]_{k_0}^{k_1}. \quad (1.48)$$

for $n \neq 3$, and $T = A^{-1/2} \ln(k_1/k_0)$ for $n = 3$.

In two and three dimensions:

$$\boxed{\begin{aligned} T_{2d} &\sim \eta^{-1/3} \ln(k_1/k_0), \\ T_{3d} &\sim \varepsilon^{-1/3} k_0^{-2/3} \end{aligned}}. \quad (1.49a,b)$$

As $k_1 \rightarrow \infty$, that is as the initial error is confined to smaller and smaller scales, predictability time grows larger for two dimensional turbulence (and for $n \geq 3$ in general), but remains finite for three dimensional turbulence.

1.5 * SPECTRUM OF A PASSIVE TRACER

$$\frac{D\phi}{Dt} = F[\phi] + \kappa \nabla^2 \phi, \quad (1.50)$$

where $F[\phi]$ is the stirring of the dye, and κ is its diffusivity

Prandtl number: $\sigma \equiv \nu/\kappa$.

If the dye is stirred at a rate χ then

$$\mathcal{K}_\chi \chi \propto \frac{\mathcal{P}(k)k}{\tau_k}, \quad (1.51)$$

where $\mathcal{P}(k)$ is the spectrum of the tracer, k is the wavenumber, τ_k is an eddy timescale and \mathcal{K}_χ is a constant, not necessarily the same constant in all cases.

Assume that τ_k is given by

$$\tau_k = [k^3 \mathcal{E}(k)]^{-1/2}. \quad (1.52)$$

If energy spectrum $\mathcal{E}(k) = Ak^{-n}$, then (1.51) becomes

$$\mathcal{K}_\chi \chi = \frac{\mathcal{P}(k)k}{[Ak^{3-n}]^{-1/2}}, \quad (1.53)$$

and

$$\boxed{\mathcal{P}(k) = \mathcal{K}_\chi A^{-1/2} \chi k^{(n-5)/2}}. \quad (1.54)$$

If the energy spectrum is steeper than -3 we use

$$\tau_k = \left[\int_{k_0}^k p^2 \mathcal{E}(p) dp \right]^{-1/2}, \quad (1.55)$$

Shallow spectrum — gives same as before. If steeper than -3 then

$$\tau_k = [k_0^3 E(k_0)]^{-1/2} \quad (1.56)$$

and

$$\boxed{\mathcal{P}(k) = \mathcal{K}'_{\chi} \chi \tau_{k_0} k^{-1}}, \quad (1.57)$$

Tracer cascade is always to smaller scales.

1.5.1 Examples

Energy inertial range flow in three dimensions

If $A = \mathcal{K}\varepsilon^{2/3}$ then tracer spectrum

$$\mathcal{P}(k) = \mathcal{K}_\chi^{3d} \varepsilon^{-1/3} \chi k^{-5/3}. \quad (1.58)$$

Experiments confirm. $\mathcal{K}_\chi^{3d} \approx 0.5 - 0.6$ in three dimensions.

Inverse energy-cascade range in two-dimensional turbulence

The tracer spectrum is then

$$\mathcal{P}(k) = \mathcal{K}_\chi^{2d} \varepsilon^{-1/3} \chi k^{-5/3}, \quad (1.59)$$

the same as (1.58), although ε is now the energy cascade rate to larger scales and the constant \mathcal{K}_χ^{2d} does not necessarily equal \mathcal{K}_χ^{3d} .

Enstrophy inertial range in two-dimensional turbulence

In the forward enstrophy inertial range the eddy timescale is $\tau_k = \eta^{-1/3}$ (assuming of course that the classical phenomenology holds). Directly from (1.51) the corresponding tracer spectrum is then

$$\mathcal{P}(k) = \mathcal{K}_\chi^{2d*} \eta^{-1/3} \chi k^{-1}. \quad (1.60)$$

The passive tracer spectrum now has the same slope as the spectrum of vorticity variance (i.e., the enstrophy spectrum), which is perhaps comforting since the tracer and vorticity obey similar equations in two dimensions.

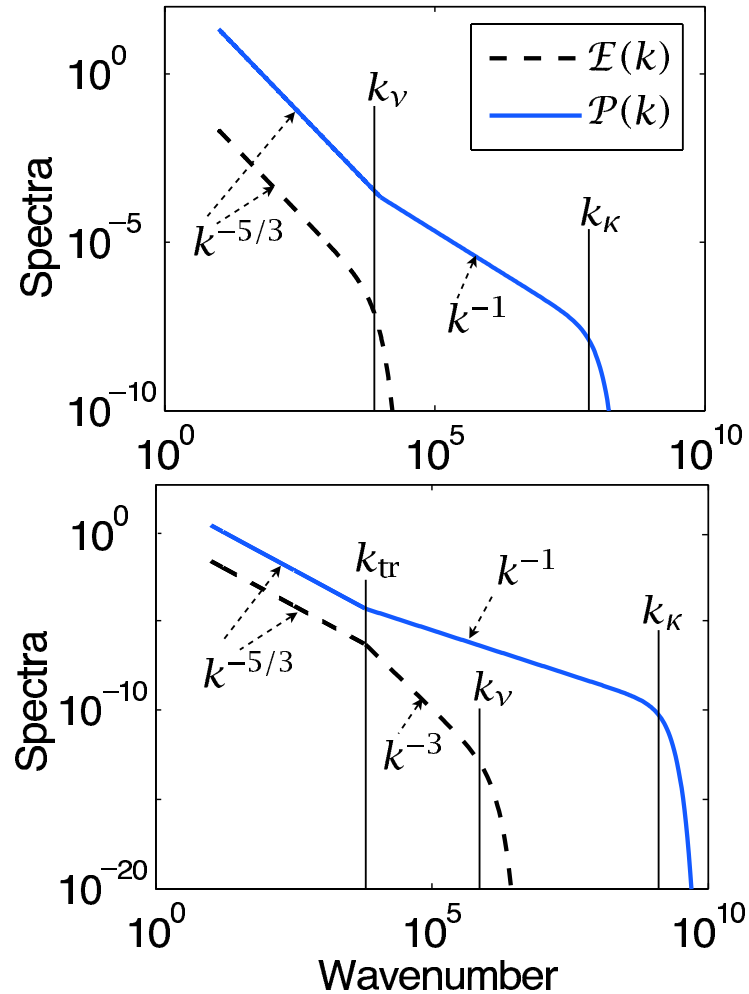


Fig. 1.10 The energy spectra, $\mathcal{E}(k)$ and passive tracer spectra $\mathcal{P}(k)$ in large Prandtl number three-dimensional turbulence (top) and two-dimensional turbulence (bottom).

CHAPTER
TWO

Geostrophic Turbulence

2.1 DIFFERENTIAL ROTATION IN TWO-DIMENSIONAL TURBULENCE

With rotation:

$$\frac{Dq}{Dt} = 0 \quad (2.1)$$

where $q = \zeta + f$.

Let $f = f_0 + \beta y$.

$$\frac{D}{Dt}(\zeta + \beta y) = 0 \quad \text{or} \quad \frac{D\zeta}{Dt} + \beta v = 0. \quad (2.2a,b)$$

If β is big, $\beta v = 0$. Flow is *zonal*.

2.1.1 Scaling

$$\frac{\partial \zeta}{\partial t} + \mathbf{u} \cdot \nabla \zeta + \beta v = 0. \quad (2.3)$$

Scales as

$$\frac{U}{LT} \quad \frac{U^2}{L^2} \quad \beta U \quad (2.4)$$

The cross-over scale, or the ' β -scale' or 'Rhines scale' L_β , is given by

$$\boxed{L_\beta \sim \sqrt{\frac{U}{\beta}}, \quad k_\beta \sim \sqrt{\frac{\beta}{U}}} \quad (2.5)$$

Alternatively, $\zeta \sim Z$ and

$$\frac{Z}{T} : \frac{UZ}{L} : \beta U \quad (2.6)$$

Equating the second and third terms gives the scale

$$L_{\beta Z} = \frac{Z}{\beta}. \quad (2.7)$$

Better:

The eddy-turnover time is

$$\tau_{\text{turbulence}} = \varepsilon^{-1/3} k^{-2/3}, \quad (2.8)$$

$$\tau_{\beta} = \frac{k}{\beta} \quad (2.9)$$

gives

$$k_{\beta} \sim \left(\frac{\beta^3}{\varepsilon} \right)^{1/5}. \quad (2.10)$$

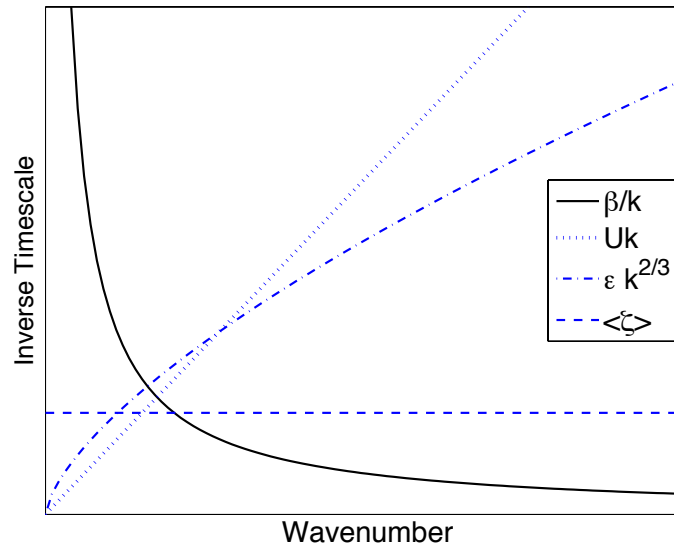


Fig. 2.1 Three estimates of the wave-turbulence cross-over, in wavenumber space. Where the Rossby wave frequency is larger (smaller) than the turbulent frequency, i.e., at large (small) scales, Rossby waves (turbulence) dominate the dynamics.

Anisotropy

$$\omega_\beta = -\frac{\beta k^x}{k^{x^2} + k^{y^2}} \quad \Omega_{\text{turbulence}} \sim \varepsilon^{1/3} k^{2/3} \quad (2.11)$$

$$\varepsilon^{1/3} k^{2/3} = \frac{\beta k^x}{k^2} \quad (2.12)$$

where k is the isotropic wavenumber. Solving this gives expressions for the x- and y-wavenumber components of the wave-turbulence boundary, namely

$$k_\beta^x = \left(\frac{\beta^3}{\varepsilon}\right)^{1/5} \cos^{8/5} \theta, \quad k_\beta^y = \left(\frac{\beta^3}{\varepsilon}\right)^{1/5} \sin \theta \cos^{3/5} \theta, \quad (2.13)$$

$$\theta = \tan^{-1}(k^y/k^x).$$

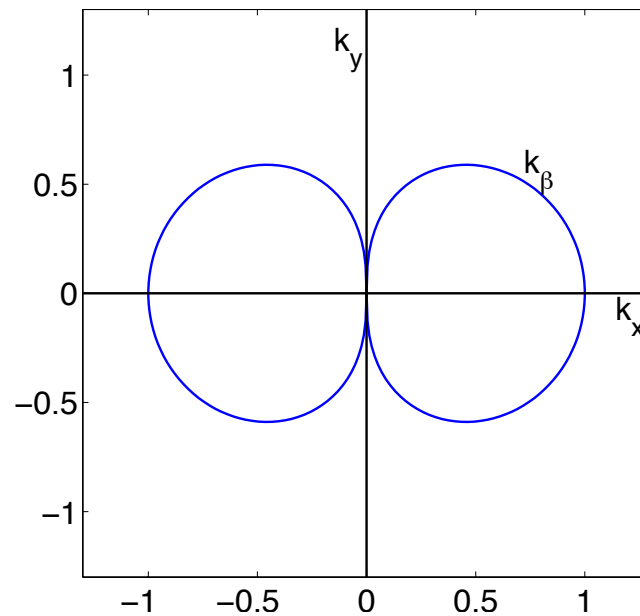
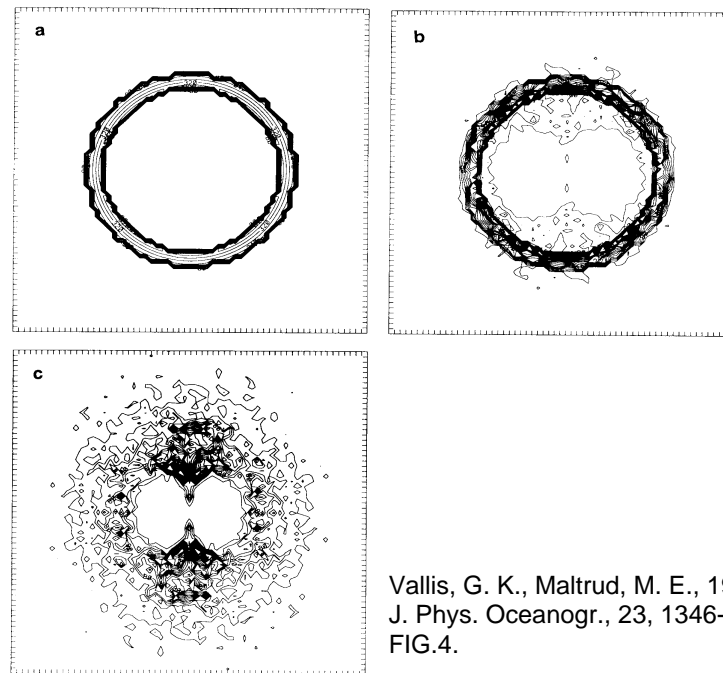


Fig. 2.2 The anisotropic wave-turbulence boundary k_β , in wave-vector space calculated by equating the turbulent eddy transfer rate, proportional to $k^{2/3}$ in a $k^{-5/3}$ spectrum, to the Rossby wave frequency $\beta k^x/k^2$, as in (2.13).



Vallis, G. K., Maltrud, M. E., 1993:
J. Phys. Oceanogr., 23, 1346--1362
FIG.4.

Fig. 2.3 Evolution of the energy spectrum in a freely-evolving two-dimensional simulation on the β -plane.

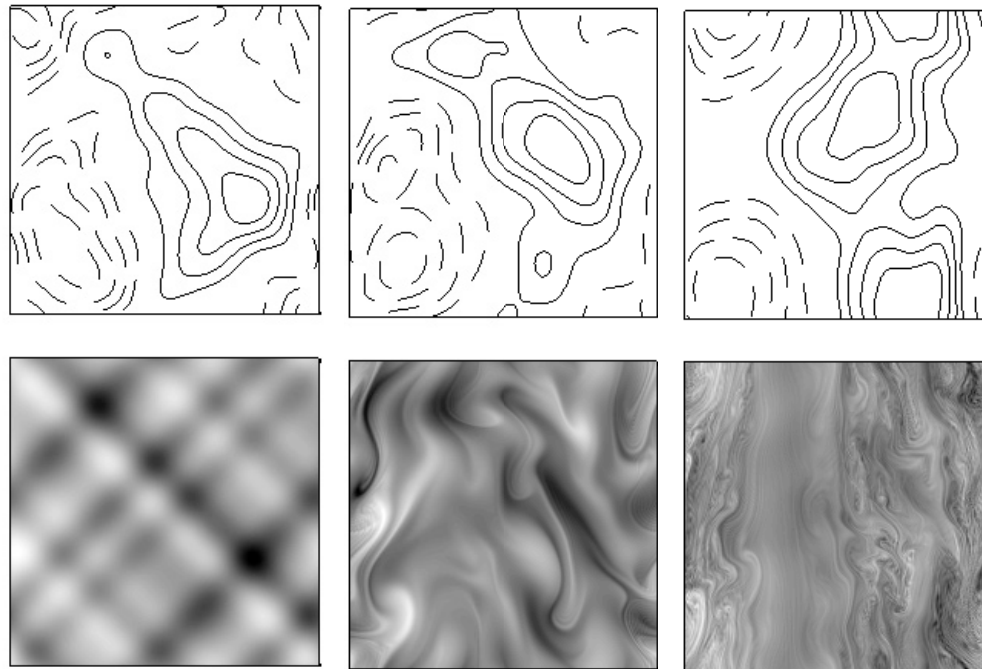


Fig. 2.4 Evolution of vorticity (greyscale, left column) and streamfunction (contour plots, right column) in physical space.

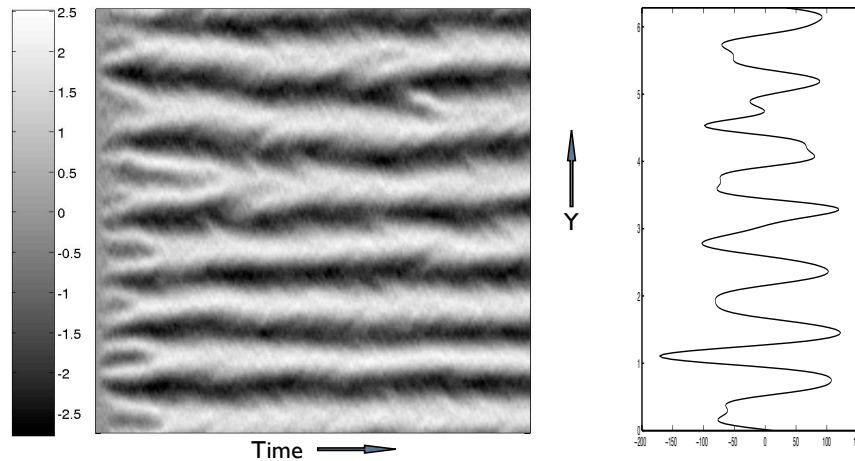


Fig. 2.5 Left: Gray-scale image of zonally average zonal velocity (\bar{u}) as a function of time and latitude (Y), produced in a simulation forced around wavenumber 80 and with $k_\beta = \sqrt{\beta/U} \approx 10$ (in a domain of size 2π). Right: Values of $\partial^2 \bar{u} / \partial y^2$ as a function of latitude, late in the integration. Jets form very quickly from the random initial conditions, and are subsequently quite steady.

2.2 STRATIFIED GEOSTROPHIC TURBULENCE

2.2.1 Quasi-geostrophic flow as an analogue to two-dimensional flow

Now let us consider stratified effects in a simple setting, namely the quasi-geostrophic equations with constant Coriolis parameter and constant stratification. The (dimensional) unforced and inviscid governing equation may then be written

$$\frac{Dq}{Dt} = 0, \quad q = \nabla^2 \psi + Pr^2 \frac{\partial^2 \psi}{\partial z^2}, \quad (2.14a)$$

where $Pr = f_0/N$. (D/Dt is *two-dimensional*).

Boundary conditions

$$\frac{D}{Dt} \left(\frac{\partial \psi}{\partial z} \right) = 0, \quad \text{at } z = 0, H. \quad (2.14b)$$

Two quadratic invariants of the motion:

$$\begin{aligned} \frac{d\hat{E}}{dt} &= 0, & \hat{E} &= \int_V \left[(\nabla \psi)^2 + Pr^2 \left(\frac{\partial \psi}{\partial z} \right)^2 \right] dV, \\ \frac{d\hat{Z}}{dt} &= 0, & \hat{Z} &= \int_V q^2 dV = \int_V \left[\nabla^2 \psi + Pr^2 \left(\frac{\partial^2 \psi}{\partial z^2} \right) \right]^2 dV. \end{aligned} \quad (2.15)$$

2.2.2 Two-layer flow

$$\frac{\partial q_i}{\partial t} + J(\psi_i, q_i) = 0, \quad i = 1, 2, \quad (2.16)$$

where (if $\beta = 0$)

$$q_1 = \nabla^2 \psi_1 + \frac{1}{2} k_d^2 (\psi_2 - \psi_1), \quad q_2 = \nabla^2 \psi_2 + \frac{1}{2} k_d^2 (\psi_1 - \psi_2), \quad (2.17a)$$

$$J(a, b) = \frac{\partial a}{\partial x} \frac{\partial b}{\partial y} - \frac{\partial b}{\partial y} \frac{\partial a}{\partial x}, \quad \frac{1}{2} k_d^2 = \frac{2f_0^2}{g'H} \equiv \frac{4f_0^2}{N^2 H^2}. \quad (2.17b)$$

$$\frac{d\hat{E}}{dt} = 0, \quad \hat{E} = \frac{1}{2} \int \left[(\nabla \psi_1)^2 + (\nabla \psi_2)^2 + \frac{1}{2} k_d^2 (\psi_1 - \psi_2)^2 \right] dA, \quad (2.18)$$

$$\frac{d\hat{Z}_1}{dt} = 0, \quad \hat{Z}_1 = \int_A q_1^2 dA, \quad (2.19)$$

$$\frac{d\hat{Z}_2}{dt} = 0, \quad \hat{Z}_2 = \int_A q_2^2 dA. \quad (2.20)$$

Baroclinic and barotropic decomposition

Define the barotropic and barotropic streamfunctions by

$$\psi \equiv \frac{1}{2}(\psi_1 + \psi_2), \quad \tau \equiv \frac{1}{2}(\psi_1 - \psi_2). \quad (2.21)$$

Then

$$\frac{\partial}{\partial t} \nabla^2 \psi + J(\psi, \nabla^2 \psi) + J(\tau, (\nabla^2 - k_d^2)\tau) = 0 \quad (2.22a)$$

$$\frac{\partial}{\partial t} (\nabla^2 - k_d^2)\tau + J(\tau, \nabla^2 \psi) + J(\psi, (\nabla^2 - k_d^2)\tau) = 0 \quad (2.22b)$$

Triad interactions:

$$\boxed{(\psi, \psi) \rightarrow \psi, \quad (\tau, \tau) \rightarrow \psi, \quad (\psi, \tau) \rightarrow \tau} . \quad (2.23)$$

Pseudo-wavenumber for baroclinic mode, τ :

$$\nabla^2 \rightarrow \nabla^2 - k_d^2, \quad k^2 \rightarrow k^2 + k_d^2 \quad (2.24)$$

Conservation properties

$$\hat{T} = \int_A (\nabla\psi)^2 dA, \quad \frac{d\hat{T}}{dt} = \int_A \psi J(\tau, (\nabla^2 - k_d^2)\tau) dA \quad (2.25a)$$

$$\hat{C} = \int_A [(\nabla\tau)^2 + k_d^2\tau^2] dA, \quad \frac{d\hat{C}}{dt} = \int_A \tau J(\psi, (\nabla^2 - k_d^2)\tau) dA. \quad (2.25b)$$

$$\frac{d\hat{E}}{dt} = \frac{d}{dt}(\hat{T} + \hat{C}) = 0. \quad (2.26)$$

Enstrophy:

$$\frac{d\hat{Z}}{dt} = 0, \quad \hat{Z} = \int_A (\nabla^2\psi)^2 + [(\nabla^2 - k_d^2)\tau]^2 dA. \quad (2.27)$$

Spectra:

$$\hat{T} = \int \mathcal{T}(k) dk \quad \text{and} \quad \hat{C} = \int \mathcal{C}(k) dk, \quad (2.28)$$

$$\hat{Z} = \int \mathcal{Z}(k) dk = \int [k^2\mathcal{T}(k) + (k^2 + k_d^2)\mathcal{C}(k)] dk. \quad (2.29)$$

2.2.3 Approximations to the equations

$$\frac{\partial}{\partial t} \nabla^2 \psi + J(\psi, \nabla^2 \psi) = -J(\tau, (\nabla^2 - k_d^2)\tau) + D[\psi], \quad (2.30a)$$

$$\frac{\partial}{\partial t} (\nabla^2 - k_d^2)\tau + J(\tau, \nabla^2 \psi) + J(\psi, (\nabla^2 - k_d^2)\tau) + U \frac{\partial}{\partial x} (\nabla^2 \psi + k_d^2 \psi) = D[\tau]. \quad (2.30b)$$

At large scales Baroclinic Mode

$$\frac{\partial}{\partial t} (-k_d^2 \tau) + J(\psi, -k_d^2 \tau) = 0 \quad (2.31)$$

or

$$\frac{\partial \tau}{\partial t} + J(\psi, \tau) = 0, \quad \frac{\partial \tau}{\partial t} + \mathbf{u} \cdot \nabla \tau = 0. \quad (2.32)$$

2.2.4 Triad interactions

Barotropic triads: As if $\tau = 0$

$$\text{Energy:} \quad \frac{d}{dt} (\mathcal{J}(k) + \mathcal{J}(p) + \mathcal{J}(q)) = 0, \quad (2.33)$$

$$\text{Enstrophy:} \quad \frac{d}{dt} (k^2 \mathcal{J}(k) + p^2 \mathcal{J}(p) + q^2 \mathcal{J}(q)) = 0. \quad (2.34)$$

Baroclinic triads: Two baroclinic wavenumbers (say p, q) interacting with a barotropic wavenumber (say k).

$$\text{Energy:} \quad \frac{d}{dt} (\mathcal{J}(k) + \mathcal{C}(p) + \mathcal{C}(q)) = 0, \quad (2.35a)$$

$$\text{Enstrophy:} \quad \frac{d}{dt} (k^2 \mathcal{J}(k) + (p^2 + k_d^2) \mathcal{C}(p) + (q^2 + k_d^2) \mathcal{C}(q)) = 0. \quad (2.35b)$$

Four cases of baroclinic triad:

- I. $(\rho, q) \gg k_d$. Then neglect k_d^2 in (2.35a) and (2.35b), and a baroclinic triad behaves like a barotropic triad, for (2.35b) is similar to (2.34). Alternatively, but equivalently, reconsider the layer form of the equations,

$$\frac{\partial q_i}{\partial t} + J(\psi_i, q_i) = 0 \quad (2.36)$$

where

$$q_i = \nabla^2 \psi_i + k_d^2(\psi_j - \psi_i) \approx \nabla^2 \psi_i \quad i = 1, 2, j = 3 - i \quad (2.37)$$

In this case, each layer is decoupled from the other.

- II. $(\rho, q, k) \ll k_d$. The energy and enstrophy conservation laws collapse to:

$$\frac{d}{dt} (\mathcal{C}(\rho) + \mathcal{C}(q)) = 0. \quad (2.38)$$

Energy is conserved among the baroclinic modes alone. No constraint preventing the transfer of baroclinic energy to smaller scales, and no production of barotropic energy at $k \ll k_d$.

Equation of motion is

$$\frac{\partial}{\partial t} (-k_d^2 \tau) + J(\psi, -k_d^2 \tau) = 0 \quad (2.39)$$

or

$$\frac{\partial \tau}{\partial t} + J(\psi, \tau) = 0, \quad \frac{\partial \tau}{\partial t} + \mathbf{u} \cdot \nabla \tau = 0. \quad (2.40)$$

τ is advected like a passive tracer.

III. $(p, q, k) \sim k_d$. Both baroclinic and barotropic modes are important. Let $k'^2 \equiv k^2 + k_d^2$ for a baroclinic mode and $k'^2 = k^2$ for a barotropic mode, and similarly for p' and q' . Then

$$\frac{d}{dt} (\mathcal{E}(k) + \mathcal{E}(p) + \mathcal{E}(q)) = 0, \quad (2.41a)$$

$$\frac{d}{dt} (k'^2 \mathcal{E}(k) + p'^2 \mathcal{E}(p) + q'^2 \mathcal{E}(q)) = 0 \quad (2.41b)$$

Energy seek the gravest (smallest pseudo-wavenumber) mode. Since the gravest mode has $k_d = 0$ this implies a *barotropization* of the flow.

IV. *Baroclinic Instability.*

$p \ll (k, q, k_d)$. The conservation laws are,

$$\begin{aligned} \frac{d}{dt} (\mathcal{J}(k) + \mathcal{C}(p) + \mathcal{C}(q)) &= 0, \\ \frac{d}{dt} (k^2 \mathcal{J}(k) + k_d^2 \mathcal{C}(p) + (q^2 + k_d^2) \mathcal{C}(q)) &= 0. \end{aligned} \quad (2.42)$$

From these, and with $k^2 \approx q^2$, we derive

$$k^2 \dot{\mathcal{C}}(q) = (k_d^2 - k^2) \dot{\mathcal{J}}(k). \quad (2.43)$$

$$k^2 < k_d^2. \quad (2.44)$$

Thus, there is a *high-wavenumber cut-off* for baroclinic instability.

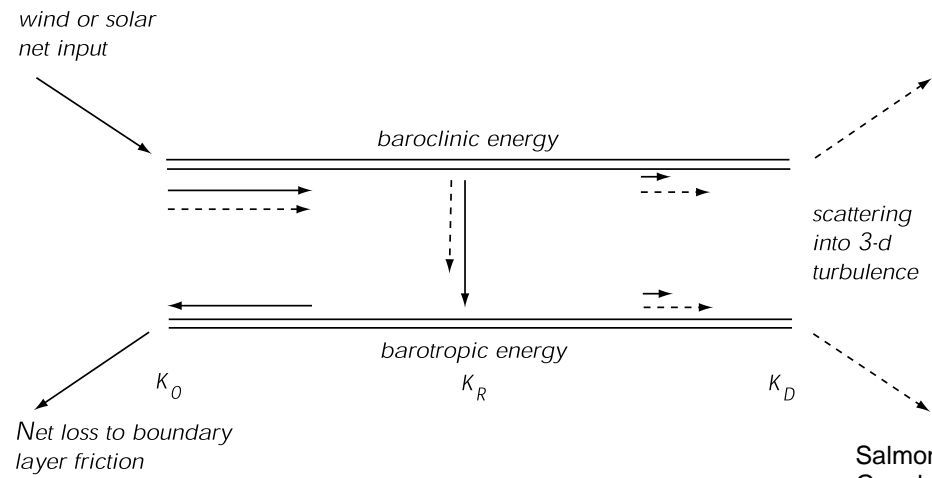


Fig. 2.6 Idealized two-layer baroclinic turbulence.

Salmon, R., 1980:
Geophys. Astrophys. Fluid Dynamics,
15, 167--211. FIG.1.

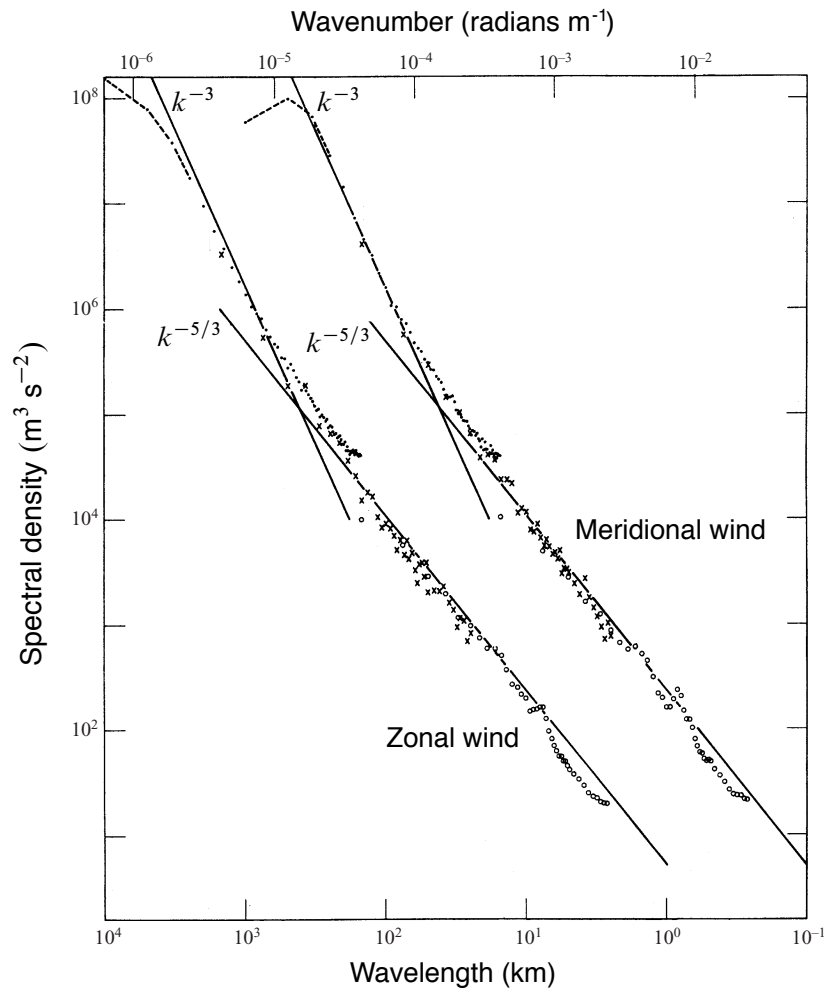


Figure 2.7 Energy spectra of the zonal and meridional wind near the tropopause, from thousands of commercial aircraft measurements between 1975 and 1979. The meridional spectrum is shifted one decade to the right. (From Gage and Nastrom 1986)

Gage, K. S., Nastrom, G. D., 1986:
J. Atmos. Sci., 43, 729--740. FIG.2.

2.3 SCALING THEORY

2.3.1 Preliminaries

Equations with shear:

$$\frac{\partial}{\partial t} \nabla^2 \psi + J(\psi, \nabla^2 \psi) + J(\tau, (\nabla^2 - k_d^2)\tau) + U \frac{\partial}{\partial x} \nabla^2 \tau = D[\psi], \quad (2.45a)$$

$$\frac{\partial}{\partial t} (\nabla^2 - k_d^2)\tau + J(\tau, \nabla^2 \psi) + J(\psi, (\nabla^2 - k_d^2)\tau) + U \frac{\partial}{\partial x} (\nabla^2 \psi + k_d^2 \psi) = D[\tau]. \quad (2.45b)$$

Large scales: $\nabla^2 \sim k^2 \ll k_d^2$:

$$\frac{\partial}{\partial t} \nabla^2 \psi + J(\psi, \nabla^2 \psi) = -J(\tau, \nabla^2 \tau) - U \frac{\partial}{\partial x} \nabla^2 \tau + D[\psi], \quad (2.46)$$

$$\frac{\partial \tau}{\partial t} + J(\psi, \tau) = U \frac{\partial \psi}{\partial x} + D[\tau]. \quad (2.47)$$

- (i) The equation for ψ is just the barotropic vorticity equation
- (ii) The equation for the τ is passive scalar, except for the forcing term $U \partial \psi / \partial x$.

Energy cascade to large barotropic scales with energy spectrum given by

$$\mathcal{E}_\psi(k) = \mathcal{K}_1 \varepsilon^{2/3} k^{-5/3}, \quad (2.48)$$

Baroclinic energy spectrum — passive tracer cascade to small scales:

$$\mathcal{E}_\tau(k) = \mathcal{K}_2 \varepsilon_\tau \varepsilon^{-1/3} k^{-5/3}, \quad (2.49)$$

$$\varepsilon_\tau = \varepsilon,$$

2.3.2 Scaling properties

Barotropic energy: $(\nabla\psi)^2$

Baroclinic energy: $(\nabla\tau)^2 + k_d^2\tau^2 \sim k_d^2\tau^2$

$$|\psi| \sim \frac{k_d|\tau|}{k_0} \gg |\tau|. \quad (2.50)$$

$$\frac{\partial\tau}{\partial t} + J(\psi, \tau - Uy) = 0, \quad (2.51)$$

suggests that

$$\tau \sim l' \frac{\partial\bar{\tau}}{\partial y} = -l'U \quad (2.52)$$

l' is eddy scale

Thus, at the scale k_0^{-1}

$$\tau \sim \frac{U}{k_0}, \quad v_\tau \sim U. \quad (2.53)$$

and

$$\psi \sim \frac{k_d U}{k_0^2}, \quad v_\psi \sim \frac{k_d U}{k_0}. \quad (2.54)$$

Energy Flux:

Multiplying (2.47) by $k_d^2\tau$ and integrate:

$$\frac{d}{dt} APE = \frac{1}{2} \frac{d}{dt} \int_A k_d^2 \tau^2 dA = \int_A U k_d^2 \tau \frac{\partial\psi}{\partial x} dA \quad (2.55)$$

so

$$\varepsilon = U k_d^2 \overline{\psi_x \tau} \sim \frac{U^3 k_d^3}{k_0^2}. \quad (2.56)$$

2.3.3 The halting scale and the β -effect

Let us suppose that the β -effect provides a barrier for the inverse cascade at the scale (2.10), namely $k_\beta \sim (\beta^3/\varepsilon)^{1/5}$. Using (2.56) this becomes

$$k_\beta = \frac{\beta}{Uk_d}, \quad (2.57)$$

This can also be derived by writing

$$k_\beta^2 = \frac{\beta}{v_\psi}, \quad v_\psi = \frac{k_d U}{k_\beta} \quad (2.58)$$

so that $k_\beta = \beta/(Uk_d)$.

Energy flux and the eddy diffusivity,

$$\varepsilon \sim \frac{U^5 k_d^5}{\beta^2}, \quad \kappa \sim \frac{U^3 k_d^3}{\beta^2} \quad (2.59)$$

The magnitudes of the eddies themselves are easily given using (2.54) and (2.53), whence

$$\tau \sim \frac{U^2 k_d}{\beta}, \quad v_\tau \sim U, \quad \psi \sim \frac{U^3 k_d^3}{\beta^2}, \quad v_\psi \sim \frac{U^2 k_d^2}{\beta} = U \frac{k_d}{k_\beta} \quad (2.60)$$

Using $v_\psi = \psi k_\beta$ and $k_\beta = \beta/(Uk_d)$.

2.4 * PHENOMENOLOGY

- (i) An assumption about the magnitude of the baroclinic eddies;
- (ii) An assumption relating eddy kinetic energy to eddy available potential energy;
- (iii) An assumption about the horizontal scale of the eddies.

(i) Assume

$$\boxed{b' \sim L_e |\nabla \bar{b}|}, \quad (2.61)$$

or (equivalently)

$$b' \sim L_e f \frac{\partial \bar{u}}{\partial z} \quad \text{and} \quad v'_\tau \sim \bar{u}, \quad (2.62a,b)$$

(ii) EKE = eddy APE. $v'_\psi^2 \sim (b'/N)^2$ or

$$v'_\psi \sim \frac{b'}{N}. \quad (2.63)$$

Now, $b' = f_0 \tau / H$ so

$$v_\psi = \frac{f_0 \tau}{NH} = k_d \tau. \quad (2.64)$$

(iii) $L_e \sim L_\beta$. Length scale is Rhines scale.

Consequences

Eddy amplitudes

$$v'_{\psi} \sim \frac{fL_e\bar{u}}{NH} \approx \frac{L_e\bar{u}}{L_d} \quad (2.65)$$

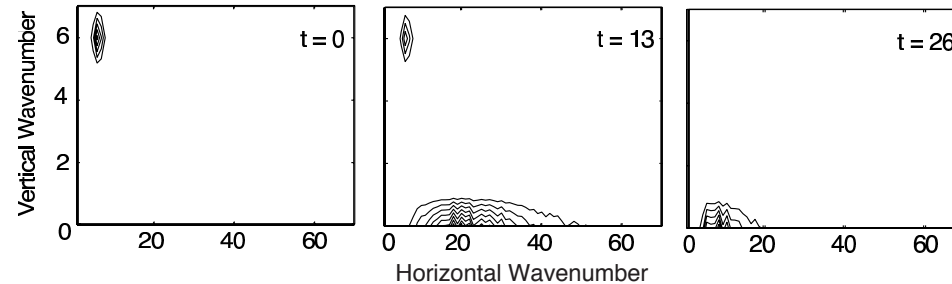
where $L_d = NH/f_0$ is the deformation radius and \bar{u} is the amplitude of the mean baroclinic velocity, that is the mean shear multiplied by the height scale.

Timescales

$$T_E \sim \frac{L_e}{v'_{\psi}} \sim \frac{L_d}{\bar{u}}, \quad (2.66)$$

and this is simply the Eady timescale. That is, the eddy timescale (at the scale of the largest eddies) is independent of the process that ultimately determines the spatial scale of those eddies; if the eddy length scale increases somehow, perhaps because friction or β are decreased, the velocity scale increases in proportion.

2.4.1 Baroclinic lifecycles

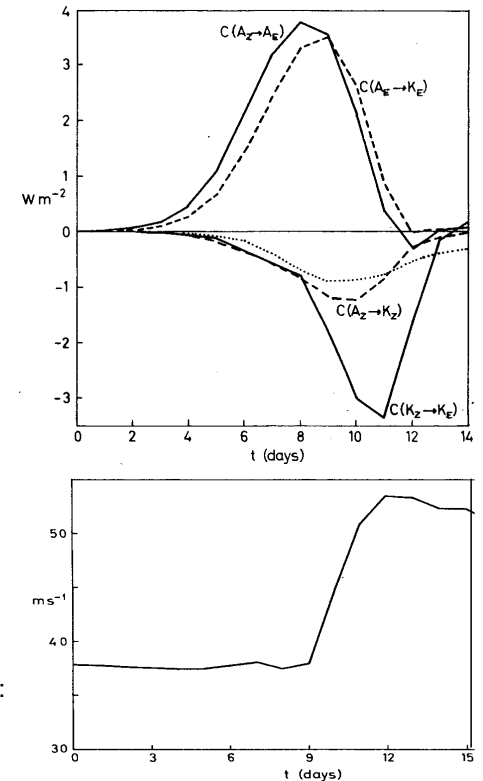


Smith, K. S., Vallis, G. K., 2001:
J. Phys. Oceanogr., 31, 554--571.
FIG.7.

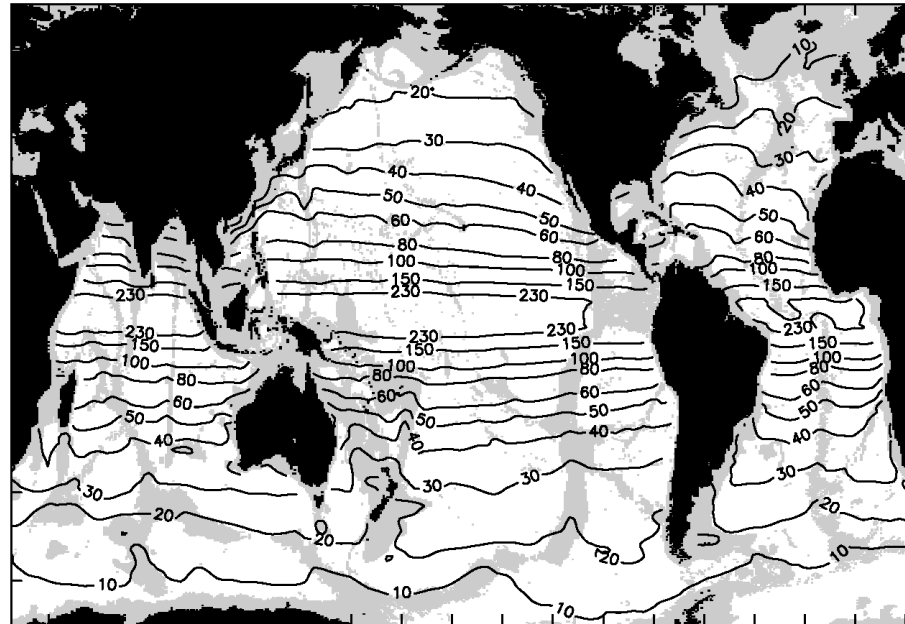
Fig. 2.8 A numerical simulation of a very idealized baroclinic lifecycle, showing contours of energy in spectral space at successive times. Initially, there is baroclinic energy at low horizontal wavenumber, as in a large-scale shear. Baroclinic instability transfers this energy to barotropic flow at the scale of the deformation radius, and this is followed by a barotropic inverse cascade to large scales. Most of the transfer to the barotropic mode in fact occurs quite quickly, between times 11 and 14, but the ensuing barotropic inverse cascade is slower. The entire process may be thought of as a generalized inverse cascade. The stratification (N^2) is uniform, and the first deformation radius is at about wavenumber 15. There is no friction in the simulation, except for a small hyperviscosity to remove small scale noise. Times are in units of eddy turnover time.

Figure 2.9 Top: Energy conversion and dissipation processes in a numerical simulation of an idealized atmospheric baroclinic lifecycle, simulated with a GCM Bottom: Evolution of the maximum zonal-mean velocity. A_Z and A_E are zonal and eddy available potential energies, and K_Z and K_E the corresponding kinetic energies. Initially baroclinic processes dominate, with conversions from zonal to eddy kinetic energy and then eddy kinetic to eddy available potential energy, followed by the barotropic conversion of eddy kinetic to zonal kinetic energy. The latter process is reflected in the *increase* of the maximum zonal-mean velocity at about day 10.

Simmons, A., Hoskins, B., 1978:
J. Atmos. Sci., 35, 414-432.
(up) FIG.5. (down) FIG.11.



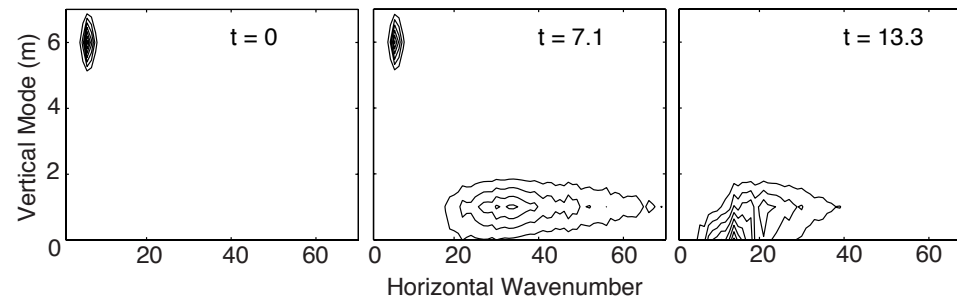
2.4.2 Baroclinic Eddies in the Ocean



Chelton, D. B., De Szoeke, R. A.,
Schlax, M. G., Naggar, K. E.,
Siwertz, N., 1998:
J. Phys. Oceanogr., 28, 433--460
FIG.6.

Fig. 2.10 The oceanic first deformation radius L_d , calculated by using the observed stratification from the eigenproblem:

$\partial^2 \phi / \partial z^2 + (N^2(z)/c^2)\phi = 0$ with $\phi = 0$ at $z = 0$ and $z = -H$, where H is the ocean depth and N is the observed buoyancy frequency. The deformation radius is given by $L_d = c/f$ where c is the first eigenvalue and f is the latitudinally varying Coriolis parameter. Near equatorial regions are excluded, and regions of ocean shallower than 3500m are shaded. Variations in Coriolis parameter are responsible for much of large-scale variability, although weak stratification also reduces the deformation radius at high latitudes.



Smith, K. S., Vallis, G. K., 2001:
J. Phys. Oceanogr., 31, 554--571.
FIG.8.

Fig. 2.11 Idealized baroclinic lifecycle, similar to that in Fig. 2.8, but with enhanced stratification of the basic state in the upper domain, representing the oceanic thermocline.

CHAPTER
THREE

Eddies and the General Circulation

3.1 POTENTIAL VORTICITY FLUX

In shallow water

$$Q = \frac{\zeta + f}{h} \quad (3.1)$$

If $h = H + h'$ and $h' \ll H$, and $f = f_0 + \beta y$, then

$$Q \approx \frac{1}{H} \left[(f + \zeta) \left(1 - \frac{h'}{H} \right) \right] \quad (3.2)$$

so we define

$$q = \zeta + \beta y - (f_0 \eta / H) = \nabla^2 \psi + \beta y - k_d^2 \psi \quad (3.3)$$

where $\psi = g\eta/f_0$ and $k_d^2 = f_0^2/(gH)$.

And the meridional flux of potential vorticity:

$$\overline{v'q'} = \overline{v'\zeta'} - \frac{f_0}{H} \overline{v'h'} \quad (3.4)$$

3.2 * THE ELIASSEN-PALM FLUX

$$q = \zeta + f + \frac{f_0}{N^2} \frac{\partial b}{\partial z}, \quad b = f_0 \frac{\partial \psi}{\partial z}, \quad \zeta = \nabla^2 \psi \quad (3.5)$$

So

$$v'q' = v'\zeta' + f_0 v' \frac{\partial}{\partial z} \left(\frac{b'}{N^2} \right) \quad (3.6)$$

$$f_0 v' \frac{\partial}{\partial z} \left(\frac{b'}{N^2} \right) = f_0 \frac{\partial}{\partial z} \left(\frac{v'b'}{N^2} \right) - \frac{f_0^2}{N^2} \frac{\partial}{\partial x} \left(\frac{1}{2} \frac{\partial \psi'}{\partial z} \right)^2 \quad (3.7)$$

using $b' = f_0 \partial \psi' / \partial z$.

$$v'\zeta' = -\frac{\partial}{\partial y} u'v' + \frac{1}{2} \frac{\partial}{\partial x} (v'^2 - u'^2) \quad (3.8)$$

Thus:

$$v'q' = -\frac{\partial}{\partial y} (u'v') + \frac{\partial}{\partial z} \left(\frac{f_0}{N^2} v'b' \right) + \frac{\partial}{\partial x} \left(\frac{1}{2} (v'^2 - u'^2) - \frac{b'^2}{N^2} \right) \quad (3.9)$$

$$\boxed{\overline{v'q'} = -\frac{\partial}{\partial y} \overline{u'v'} + \frac{\partial}{\partial z} \left(\frac{f_0}{N^2} \overline{v'b'} \right)} \quad (3.10)$$

Eliassen-Palm flux

$$\mathcal{F} \equiv -\overline{u'v'} \mathbf{j} + \frac{f_0}{N^2} \overline{v'b'} \mathbf{k} \quad (3.11)$$

So that:

$$\overline{v'q'} = \nabla \cdot \mathcal{F} \quad (3.12)$$

3.2.1 Eliassen-Palm relation

Linear PV:

$$\frac{\partial q'}{\partial t} + \bar{u} \frac{\partial q'}{\partial x} + v' \frac{\partial \bar{q}}{\partial y} = D', \quad (3.13)$$

Enstrophy equation:

$$\frac{1}{2} \frac{\partial \overline{q'^2}}{\partial t} = -\overline{v'q'} \frac{\partial \bar{q}}{\partial y} + \overline{D'q'}. \quad (3.14)$$

So we get the *Eliassen-Palm relation*:

$$\boxed{\frac{\partial A}{\partial t} + \nabla \cdot \mathcal{F} = \mathcal{D}}, \quad (3.15a)$$

where

$$A = \frac{\overline{q'^2}}{2\partial \bar{q}/\partial y}, \quad \mathcal{D} = \frac{\overline{D'q'}}{\partial \bar{q}/\partial y} \quad (3.15b)$$

Integrate, with $\mathcal{D} = 0$

$$\frac{d}{dt} \int_A A dA = 0. \quad (3.16)$$

Pseudomomentum or wave activity conservation.

3.2.2 The group velocity property (For the keen student)

If the disturbance is composed of plane or almost plane waves then $\mathcal{F} = c_g \mathcal{A}$,

$$\frac{\partial \mathcal{A}}{\partial t} + \nabla \cdot (\mathcal{A} \mathbf{c}_g) = 0. \quad (3.17)$$

$$\left(\frac{\partial}{\partial t} + \bar{u} \frac{\partial}{\partial x} \right) \left[\nabla^2 \psi' + \frac{\partial}{\partial z} \left(\frac{f_0^2}{N^2} \frac{\partial \psi'}{\partial z} \right) \right] + \beta \frac{\partial \psi'}{\partial x} = 0. \quad (3.18)$$

$$\omega = \bar{u} k - \frac{\beta k}{\kappa^2}. \quad (3.19)$$

with group velocities,

$$c_g^y = \frac{2\beta k l}{\kappa^2}, \quad c_g^z = \frac{2\beta k m f_0^2 / N^2}{\kappa^2}, \quad (3.20)$$

where $\kappa^2 = (k^2 + l^2 + m^2 f_0^2 / N^2)$.

$$\tilde{u} = -ik\tilde{\psi}, \quad \tilde{v} = il\tilde{\psi}, \quad \tilde{b} = imf_0\tilde{\psi}, \quad \tilde{q} = -\kappa^2\tilde{\psi}. \quad (3.21)$$

Then

$$\mathcal{A} = \frac{1}{2} \frac{\overline{q'^2}}{\beta} = \frac{\kappa^4}{4\beta} |\tilde{\psi}^2| \quad (3.22)$$

and

$$\begin{aligned} \mathcal{F}^y &= -\overline{u'v'} = \frac{1}{2} k l |\tilde{\psi}^2| \\ \mathcal{F}^z &= \frac{f_0}{N^2} \overline{v'b'} = \frac{f_0^2}{2N^2} k m |\tilde{\psi}^2|. \end{aligned} \quad (3.23)$$

Using this in (3.20) and (3.22) gives

$$\boxed{\mathcal{F} = (\mathcal{F}^y, \mathcal{F}^z) = \mathbf{c}_g \mathcal{A}}. \quad (3.24)$$

3.3 * THE TRANSFORMED EULERIAN MEAN

$$\frac{\partial \bar{u}}{\partial t} = f_0 \bar{v} - \frac{\partial}{\partial y} \overline{u'v'} + \bar{F}, \quad (3.25a)$$

$$\frac{\partial \bar{b}}{\partial t} = -N^2 \bar{w} - \frac{\partial}{\partial y} \overline{v'b'} + \bar{J}, \quad (3.25b)$$

Define a mean meridional streamfunction ψ_m such that

$$(\bar{v}, \bar{w}) = \left(-\frac{\partial \psi_m}{\partial z}, \frac{\partial \psi_m}{\partial y} \right). \quad (3.26)$$

Also define a 'residual' streamfunction by

$$\psi^* \equiv \psi_m + \frac{1}{N^2} \overline{v'b'}, \quad (\bar{v}^*, \bar{w}^*) = \left(-\frac{\partial \psi^*}{\partial z}, \frac{\partial \psi^*}{\partial y} \right), \quad (3.27)$$

and

$$\bar{v}^* = \bar{v} - \frac{\partial}{\partial z} \left(\frac{1}{N^2} \overline{v'b'} \right), \quad \bar{w}^* = \bar{w} + \frac{\partial}{\partial y} \left(\frac{1}{N^2} \overline{v'b'} \right). \quad (3.28)$$

(3.25a) and (3.25b) become

$$\boxed{\begin{aligned} \frac{\partial \bar{u}}{\partial t} &= f_0 \bar{v}^* + \overline{v'q'} + \bar{F} \\ \frac{\partial \bar{b}}{\partial t} &= -N^2 \bar{w}^* + \bar{J} \end{aligned}}, \quad (3.29)$$

where

$$\overline{v'q'} \equiv -\frac{\partial}{\partial y} \overline{u'v'} + \frac{\partial}{\partial z} \left(\frac{f_0}{N^2} \overline{v'b'} \right). \quad (3.30)$$

3.4 TRANSFORMED EULERIAN MEAN OR TEM

3.4.1 Shallow water (isentropic coordinates)

$$\frac{\partial u}{\partial t} + \mathbf{u} \cdot \nabla u - f v = -g \frac{\partial h}{\partial x} F \quad (3.31a)$$

$$\frac{\partial h}{\partial t} + \nabla \cdot (h\mathbf{u}) = J \quad (3.31b)$$

Zonal average, QG scaling:

$$\frac{\partial \bar{u}}{\partial t} - f_0 \bar{v} = \overline{v' \zeta'} + \bar{F} \quad (3.32a)$$

$$\frac{\partial \bar{h}}{\partial t} + H \frac{\partial \bar{v}}{\partial y} = -\frac{\partial}{\partial y} \overline{v' h'} + \bar{J}[h] \quad (3.32b)$$

Define

$$\bar{v}^* = \bar{v} + \frac{1}{H} \overline{v' h'} \quad (3.33)$$

Then

$$\boxed{\begin{aligned} \frac{\partial \bar{u}}{\partial t} - f_0 \bar{v}^* &= \overline{v' q'} + \bar{F} \\ \frac{\partial \bar{h}}{\partial t} + H \frac{\partial \bar{v}^*}{\partial y} &= \bar{J}[h]. \end{aligned}} \quad (3.1a,b)$$

where

$$\overline{v' q'} = \overline{v' \zeta'} - \frac{f_0}{H} \overline{v' h'}. \quad (3.35)$$

From (3.33) we see that the residual velocity is a measure of the *total meridional mass flux*, eddy plus mean, in an isentropic layer.

We define the mass-weighted mean by

$$\bar{v}_* \equiv \frac{\overline{hv}}{\bar{h}} \quad (3.36)$$

so that

$$\bar{v}_* = \bar{v} + \frac{1}{\bar{h}} \overline{v'h'}, \quad (3.37)$$

then the zonal average of (3.31b) is just

$$\frac{\partial \bar{h}}{\partial t} + \frac{\partial}{\partial y} (\bar{h} \bar{v}_*) = \bar{J}[h], \quad (3.38)$$

which is the same as (??).

3.5 THE MAINTENANCE OF JETS IN THE ATMOSPHERE

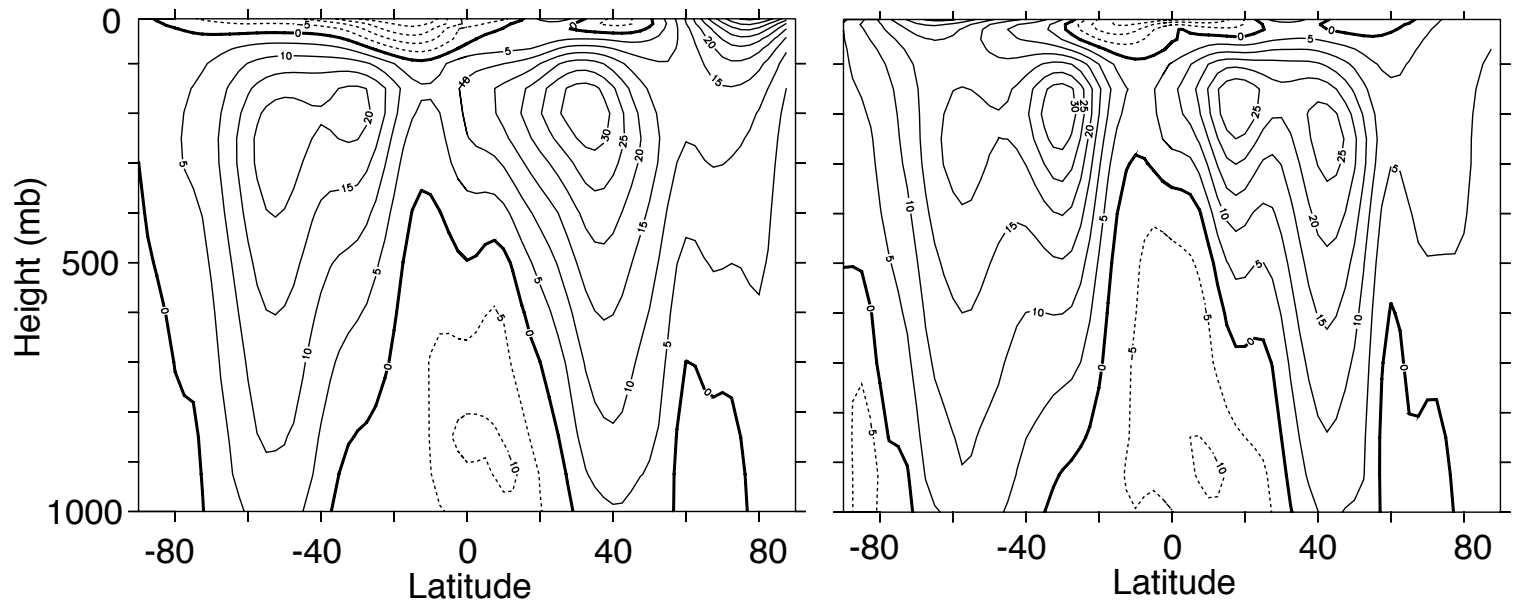


Fig. 3.1 The time-averaged zonal wind at 150°W (in the mid Pacific) in December-January February (DJF, left), March-April-May (MAM, right). The contour interval is 5 m s⁻¹. Note the double jet in each hemisphere, one in the subtropics and one in midlatitudes. The subtropical jets is associated with strong meridional temperature gradient, whereas the midlatitude jets have a stronger barotropic component and are associated with westerly winds at the surface.

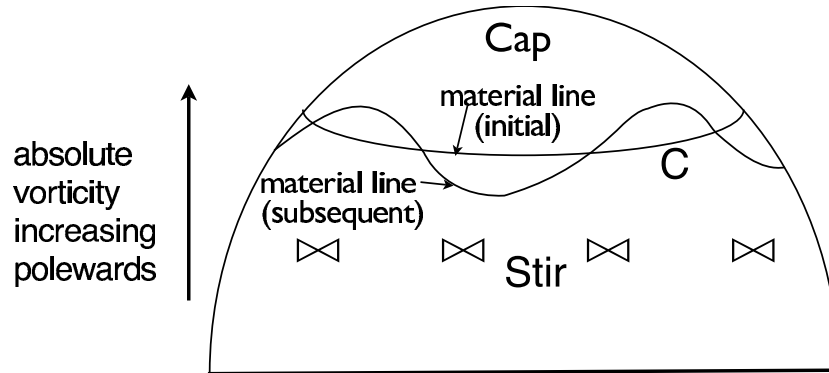


Figure 3.2 Disturbance will bring fluid with lower absolute vorticity into the cap region, and the velocity around the latitude line C will become more westward.

1. The vorticity budget

Basic state vorticity increases monotonically polewards.

Circulation around the cap

$$I_1 = \int_{\text{cap}} \boldsymbol{\omega}_{i_a} \cdot d\mathbf{A} = \oint_C u_{i_a} dl = \oint_C (u_i + 2\Omega a \cos \vartheta) dl, \tag{3.39}$$

Take $u_i = 0$

After the disturbance

$$I_f = \int_{\text{cap}} \boldsymbol{\omega}_{f_a} \cdot d\mathbf{A} < I_i \tag{3.40}$$

so that

$$\oint_C (u_f + 2\Omega a \cos \vartheta) dl < \oint_C (u_i + 2\Omega a \cos \vartheta) dl \tag{3.41}$$

and

$$\bar{u}_f < \bar{u}_i \tag{3.42}$$

with the overbar indicating a zonal average. Thus, there is a tendency to produce *westward* flow polewards of the disturbance.

II. Rossby waves and momentum flux

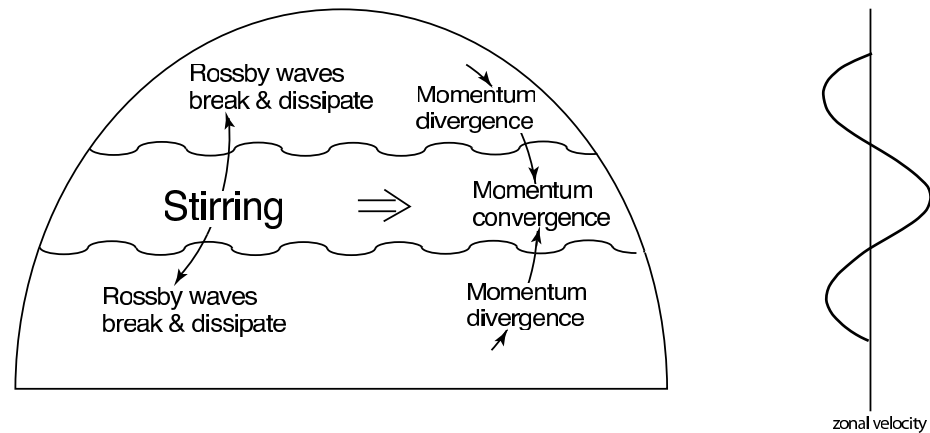


Fig. 3.3 Generation of zonal flow on a β -plane or on a rotating sphere. Stirring in generates Rossby waves that propagate away from the disturbance. Momentum converges in the region of stirring, producing eastward flow there and weaker westward flow on its flanks.

$$\psi = \text{Re } C e^{i(kx+ly-\omega t)} = \text{Re } C e^{i(kx+ly-ckt)}, \quad (3.43)$$

where C is a constant, with dispersion relation

$$\omega = ck = \bar{u}k - \frac{\beta k}{k^2 + l^2} \equiv \omega_R. \quad (3.44)$$

The meridional component of the group velocity is given by

$$c_g^y = \frac{\partial \omega}{\partial l} = \frac{2\beta kl}{(k^2 + l^2)^2}. \quad (3.45)$$

Group velocity is directed *away* from the source region.

Poleward of source: $kl > 0$ Southwards of the source $kl < 0$

The velocity variations associated with the Rossby waves are

$$u' = -\text{Re } C i l e^{i(kx+ly-\omega t)}, \quad v' = \text{Re } C i k e^{i(kx+ly-\omega t)}, \quad (3.46a,b)$$

Momentum flux is:

$$\overline{u'v'} \propto -\frac{1}{2} C^2 kl. \quad (3.47)$$

Northwards of the source $\overline{u'v'} < 0$

Southwards of the source $\overline{u'v'} > 0$

That is, the momentum flux associated with the Rossby waves is *toward* the source region. Momentum *converges* in the region of the stirring.

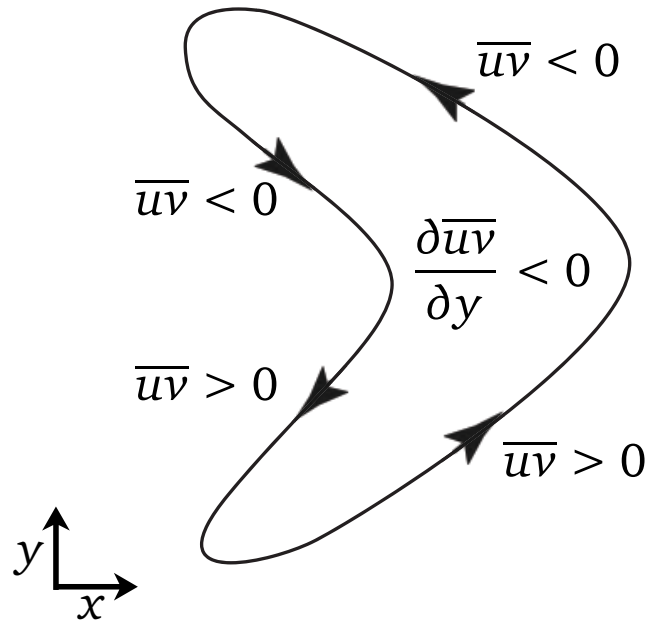


Fig. 3.4 The momentum transport in physical space, caused by the propagation of Rossby waves away from a source in midlatitudes. The ensuing bow-shaped eddies are responsible for a convergence of momentum, as indicated in the idealization pictured.

III. The pseudomomentum budget

Zonal momentum equation:

$$\frac{\partial u}{\partial t} + \frac{\partial u^2}{\partial x} + \frac{\partial uv}{\partial y} - fv = -\frac{\partial \phi}{\partial x} + F_u - D_u, \quad (3.48)$$

Zonal averaging, with $\bar{v} = 0$, gives

$$\frac{\partial \bar{u}}{\partial t} = -\frac{\partial \bar{uv}}{\partial y} + \bar{F}_u - \bar{D}_u = \overline{v'\zeta'} - r\bar{u} \quad (3.49)$$

Barotropic vorticity equation is

$$\frac{\partial \zeta}{\partial t} + \mathbf{u} \cdot \nabla \zeta + v\beta = F_\zeta - D_\zeta. \quad (3.50)$$

Linearize

$$\frac{\partial \zeta'}{\partial t} + \bar{u} \frac{\partial \zeta'}{\partial x} + \beta v' = F'_\zeta - D'_\zeta, \quad (3.51)$$

Multiply (3.51) by ζ'/β and zonally average to form the pseudomomentum equation,

$$\frac{\partial P}{\partial t} + \overline{v'\zeta'} = \frac{1}{\beta} (\overline{\zeta'F'_\zeta} - \overline{\zeta'D'_\zeta}), \quad (3.52)$$

where

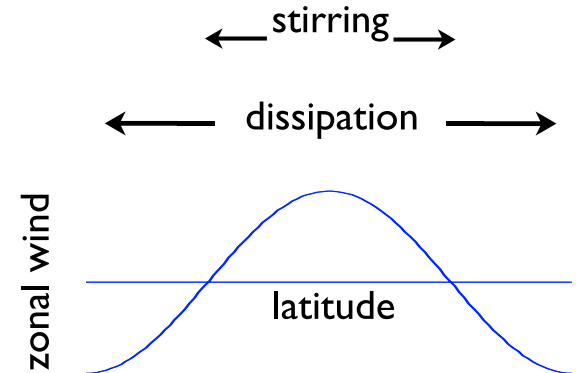
$$P = \frac{1}{2\beta} \overline{\zeta'^2} \quad (3.53)$$

is the negative of the pseudomomentum.

If $F_\zeta = D_\zeta = 0$

$$\frac{\partial \bar{u}}{\partial t} + \frac{\partial P}{\partial t} = 0. \quad (3.54)$$

Figure 3.5 Pseudomomentum stirring, which in reality occurs via baroclinic instability, is confined to midlatitudes. Because of Rossby wave propagation away from the source region, the distribution of pseudomomentum dissipation is broader, and the sum of the two leads to the zonal wind distribution shown, with positive (eastward) values in the region of the stirring. See also Fig. 3.8.



In general

$$\frac{\partial \bar{u}}{\partial t} + \frac{\partial P}{\partial t} = -r\bar{u} + \frac{1}{\gamma}(\overline{\zeta'F'_\zeta} - \overline{\zeta'D'_\zeta}), \quad (3.55)$$

If steady:

$$\boxed{r\bar{u} = \frac{1}{\gamma}(\overline{\zeta'F'_\zeta} - \overline{\zeta'D'_\zeta})}. \quad (3.56)$$

IV. The Eliassen-Palm flux

$$\frac{\partial \bar{u}}{\partial t} - f_0 \bar{v}^* = \nabla_x \cdot \mathcal{F} - r \bar{u} \quad (3.57)$$

\bar{v}^* is the residual meridional velocity

\mathcal{F} is the Eliassen-Palm (EP) flux, that obeys

$$\frac{\partial \mathcal{A}}{\partial t} + \nabla \cdot \mathcal{F} = 0, \quad \frac{\partial \mathcal{A}}{\partial t} + \nabla \cdot (\mathcal{A} c_g) = 0, \quad (3.58)$$

In the barotropic case $\bar{v}^* = 0$ and

$$\mathcal{F} = -\mathbf{j} \overline{u'v'}. \quad (3.59)$$

EP flux obeys the group velocity property:

$$\mathcal{F}^y \equiv \mathbf{j} \cdot \mathcal{F} \approx c_g^y \mathcal{A} \quad (3.60)$$

so

$$\frac{\partial \mathcal{A}}{\partial t} = -\frac{\partial}{\partial y} c_g^y \mathcal{A} = \begin{cases} < 0 & \text{in stirring region} \\ > 0 & \text{in dissipation region} \end{cases} \quad (3.61)$$

$$\frac{\partial \bar{u}}{\partial t} = -\frac{\partial \mathcal{A}}{\partial t} > 0 \quad \text{in stirring region} \quad (3.62)$$

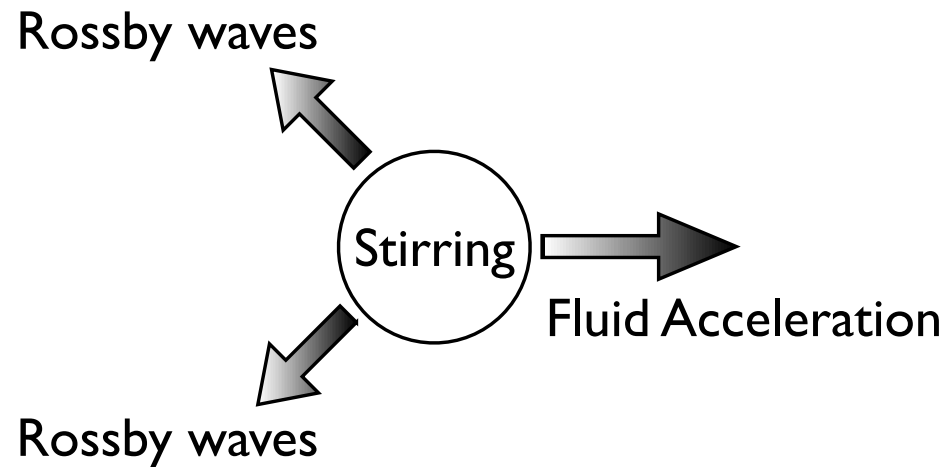


Fig. 3.6 If a region of fluid on the β -plane or on a rotating sphere is stirred, then Rossby waves will propagate westwards and away from the disturbance, and this is the direction of propagation of wave activity density. Thus, there is positive divergence of wave activity in the stirred region, and using (3.60) and (3.57) this produces a westward acceleration.

3.5.1 Numerical examples

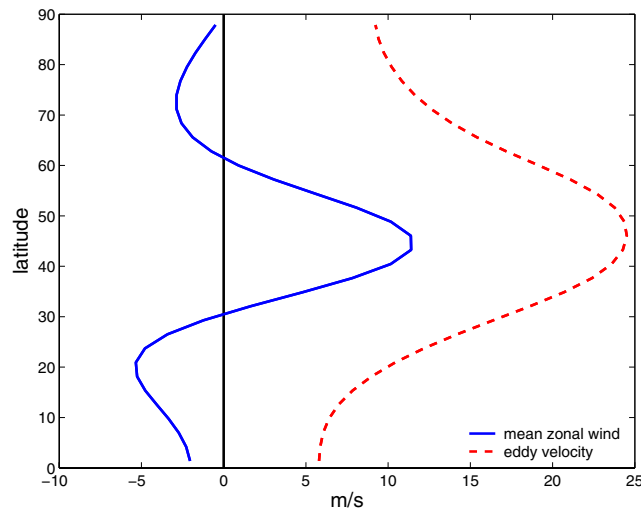


Fig. 3.7 The time- and zonally-averaged wind (solid line) obtained by an integration of the barotropic vorticity equation (??) on the sphere. The fluid is stirred in midlatitudes by a random wavemaker that is statistically zonally uniform, acting around zonal wavenumber 8, and that supplies no net momentum. Momentum converges in the stirring region leading to an eastward jet with a westward flow to either side, and zero area-weighted spatially integrated velocity. The dashed line shows the r.m.s. (eddy) velocity created by the stirring.

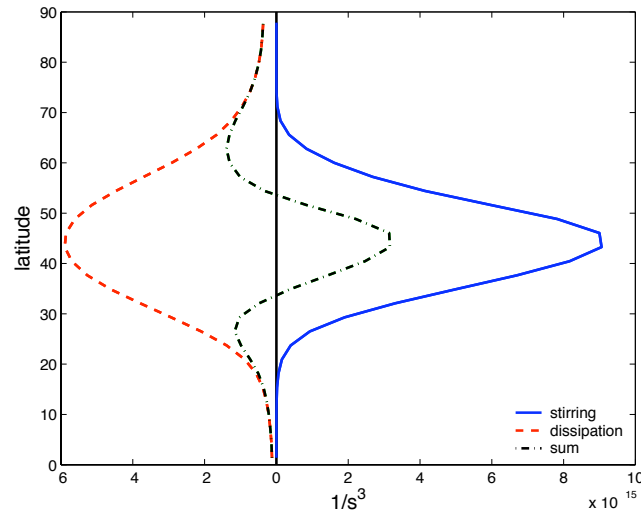


Fig. 3.8 The pseudomomentum stirring (solid line, $\overline{F'_\zeta \zeta'}$), dissipation (dashed line, $\overline{D'_\zeta \zeta'}$) and their sum (dot-dashed), for the same integration as Fig. 3.7. Because Rossby waves propagate away from the stirred region before breaking, the distribution of dissipation is broader than the forcing, resulting in an eastward jet where the stirring is centered, with westward flow on either side.

3.6 THE FERREL CELL

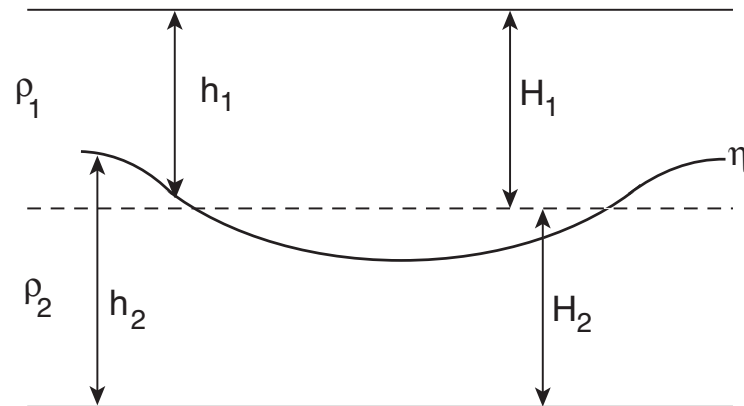


Fig. 3.9 Two homogeneous layers of mean thickness H_1 and H_2 , local thickness h_1 and h_2 , and interface η , contained between two flat, rigid surfaces.

3.6.1 Equations of motion

Zonal average:

$$\frac{\partial \bar{u}_1}{\partial t} - f_0 \bar{v}_1 = \overline{v'_1 \zeta'_1} \quad (3.63a)$$

$$\frac{\partial \bar{u}_2}{\partial t} - f_0 \bar{v}_2 = \overline{v'_2 \zeta'_2} - r \bar{u}_2, \quad (3.63b)$$

Geostrophic balance

$$f_0 \mathbf{u}_{g1} = \mathbf{k} \times \nabla \phi_T, \quad f_0 \mathbf{u}_{g2} = \mathbf{k} \times \nabla \phi_T - g' \mathbf{k} \times \nabla \eta, \quad (3.64a,b)$$

Thermal wind:

$$\boxed{f_0(\mathbf{u}_1 - \mathbf{u}_2) = g' \mathbf{k} \times \nabla \eta}, \quad (3.65)$$

Temperature gradient \implies a slope of the interface height.

Interfaces slopes upwards toward lower temperatures

$$\text{PV} \quad q_i = \zeta_i + f - f_0 \frac{h_i}{H_i} \quad (3.66)$$

$$\text{PV Fluxes:} \quad \overline{v'_i q'_i} = \overline{v'_i \zeta'_i} - \frac{f_0}{H_i} \overline{v'_i h'_i}. \quad (3.67)$$

$$\text{Residual velocity} \quad \bar{\mathbf{v}}_i^* = \bar{\mathbf{v}} + \frac{\overline{v'_i h'_i}}{H_i} \quad (3.68)$$

so that

$$\boxed{\begin{aligned} \frac{\partial \bar{u}_1}{\partial t} &= \overline{v'_1 q'_1} + f_0 \bar{v}_1^* \\ \frac{\partial \bar{u}_2}{\partial t} &= \overline{v'_2 q'_2} + f_0 \bar{v}_2^* - r \bar{u}_2 \end{aligned}}. \quad (3.69)$$

$$H_1 \bar{v}_1^* + H_2 \bar{v}_2^* = 0 \quad (3.70)$$

Mass continuity:

$$\frac{\partial \bar{h}_i}{\partial t} + \frac{\partial \bar{h}_i \bar{v}_i}{\partial y} = S_i \quad (3.71)$$

or

$$\boxed{\frac{\partial h_i}{\partial t} + H_i \frac{\partial \bar{v}_i^*}{\partial y} = S_i} \quad (3.72)$$

$$\frac{\partial S_1}{\partial y} < 0 \quad \bar{v}_1^* > 0 \quad (3.73)$$

$$\frac{\partial S_2}{\partial y} < 0 \quad \bar{v}_2^* > 0 \quad (3.74)$$

So mass flux in the upper layer moves polewards!

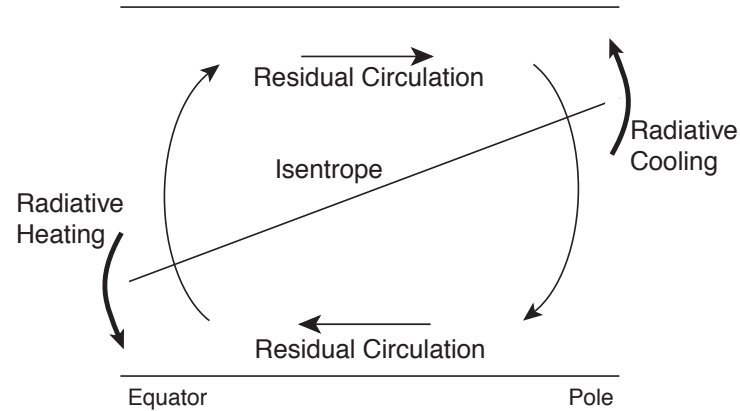


Fig. 3.10 Cooling at high latitudes and heating at low leads steepens the interface upward toward the pole (thicker arrows). Associated with this there is a net mass flux — the residual flow, or the meridional overturning circulation (lighter arrows). In the tropics this circulation is accounted for by the Hadley Cell, and is nearly all in the mean flow. In midlatitudes the circulation — the residual flow — is largely due to baroclinic eddies, and the smaller Eulerian mean flow is actually in the opposite sense.

* *Manipulations*

Interface height:

$$\frac{\partial \eta}{\partial t} + \nabla \cdot (\eta \mathbf{u}_1) = S_1, \quad \text{or} \quad \frac{\partial \eta}{\partial t} + \nabla \cdot (\eta \mathbf{u}_2) = -S_2 \quad (3.75)$$

Zonal average

$$\frac{\partial \bar{\eta}}{\partial t} - H_1 \frac{\partial \bar{v}_1^*}{\partial y} = S, \quad \text{or} \quad \frac{\partial \bar{\eta}}{\partial t} + H_2 \frac{\partial \bar{v}_2^*}{\partial y} = S \quad (3.76)$$

where $S = -S_1 = +S_2$

Using the thermal wind relationship we have

$$\overline{(v'_1 - v'_2)\eta'} = g' \frac{\partial \overline{\eta'}}{\partial x} = 0 \quad (3.77)$$

Hence, if the upper and lower surfaces are both flat, we have that

$$\overline{v'_1 h'_1} = -\overline{v'_2 h'_2} \quad (3.78)$$

Eddy meridional mass fluxes in each layer are equal and opposite.

Eqs. (3.78) and (??) are *dynamical* results, and not just kinematic ones. Form drag on each layer is equal and opposite.

$$\overline{v'_1 \eta'} = -[-\overline{v'_2 \eta'}], \quad (3.79)$$

PV Flux:

$$H_1 \overline{v'_1 q'_1} + H_2 \overline{v'_2 q'_2} = H_1 \overline{v'_1 \zeta'_1} + H_2 \overline{v'_2 \zeta'_2} = H_1 \frac{\partial}{\partial y} \overline{u'_1 v'_1} + H_2 \frac{\partial}{\partial y} \overline{u'_2 v'_2}, \quad (3.80)$$

and integrating with respect to y between quiescent latitudes gives

$$\int \left[H_1 \overline{v'_1 q'_1} + H_2 \overline{v'_2 q'_2} \right] dy = 0 \quad (3.81)$$

3.6.2 Surface Wind

From (3.69),

$$rH_2\bar{u}_2 = H_1\overline{v_1'q_1'} + H_2\overline{v_2'q_2'} = H_1\overline{v_1'\zeta_1'} + H_2\overline{v_2'\zeta_2'} \quad (3.82)$$

using (??).

$$\frac{\partial q_1}{\partial y} = \beta - \frac{f_0}{H_1} \frac{\partial \bar{h}_1}{\partial y} \gg 0 \quad (3.83a)$$

and

$$\frac{\partial q_2}{\partial y} = \beta - \frac{f_0}{H_2} \frac{\partial \bar{h}_2}{\partial y} \lesssim 0. \quad (3.83b)$$

Rossby waves will propagate further in the upper layer, and this asymmetry is the key to the production of surface winds.

I. Rossby waves and the vorticity flux

The stronger potential vorticity gradient of the upper layer is better able to support linear Rossby waves than the lower layer. Thus, the vorticity flux in the region of Rossby-wave genesis in midlatitudes will be large and positive in the upper layer, and small and negative in the lower layer.

II. Potential vorticity flux

Now, the pseudomomentum equation for each layer is

$$\frac{\partial P_i}{\partial t} = \frac{\partial}{\partial t} \left(\frac{\overline{q_i'^2}}{2\gamma_i} \right) = -\overline{v_i'q_i'} - \frac{\overline{D_i'q_i'}}{\gamma_i}, \quad i = 1, 2. \quad (3.84)$$

where γ_i , the potential vorticity gradient, has opposite signs in each layer. In a statistically steady state, the region of strongest dissipation is the region where the potential vorticity flux is be most negative.

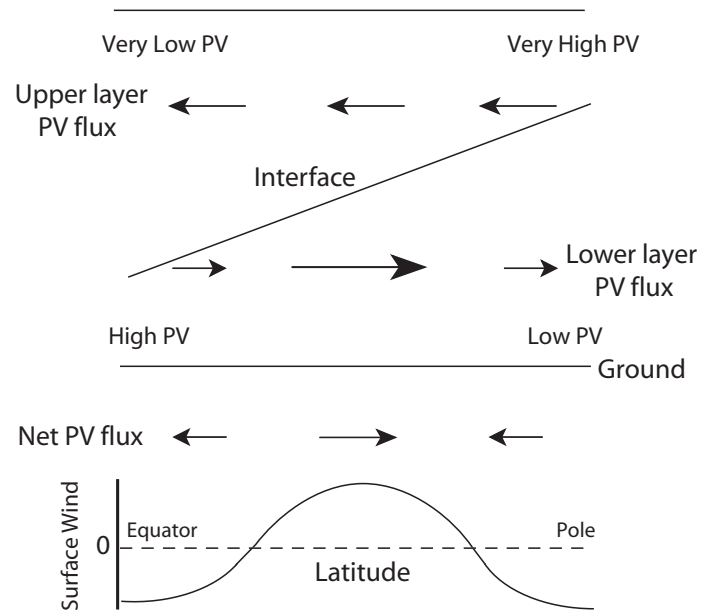


Fig. 3.11 Sketch of the potential vorticity fluxes in a two-layer model. The surface wind is proportional to their vertical integral. The PV fluxes are negative (positive) in the upper (lower) layer, but are more uniformly distributed at upper levels. The lower panel shows the net (vertically integrated) PV fluxes, and the associated surface winds.

Phenomenology of a Two-layer Mid-latitude Atmosphere: a Summary

Potential vorticity gradients in each layer are given by

$$\frac{\partial \bar{q}_1}{\partial y} = \beta - \frac{f_0}{H_1} \frac{\partial \bar{h}_1}{\partial y} > 0 \quad \text{and} \quad \frac{\partial \bar{q}_2}{\partial y} = \beta - \frac{f_0}{H_2} \frac{\partial \bar{h}_2}{\partial y} \lesssim 0. \quad (\text{TL.1})$$

The gradient is large and positive in upper layer and small and negative in the lower layer — the gradient must change sign if there is to be baroclinic instability which we assume to be the case.

$$\frac{\partial \bar{u}_1}{\partial t} = f_0 \bar{v}_1 + \overline{v'_1 \zeta'_1} = f_0 \bar{v}_1^* + \overline{v'_1 q'_1} \quad (\text{TL.2a})$$

$$\frac{\partial \bar{u}_2}{\partial t} = f_0 \bar{v}_2 + \overline{v'_2 \zeta'_2} - r \bar{u}_2 = f_0 \bar{v}_2^* + \overline{v'_2 q'_2} - r \bar{u}_2 \quad (\text{TL.2b})$$

In steady state the potential vorticity flux will be equatorward in the upper layer and poleward in the lower layer.

$$r H_1 \bar{u}_1 = H_1 \overline{v'_1 q'_1} + H_2 \overline{v'_2 q'_2} = H_1 \overline{v'_1 \zeta'_1} + H_2 \overline{v'_2 \zeta'_2} \quad (\text{TL.3})$$

Because the potential vorticity gradient in the upper layer is large, this layer is more linear than the lower layer and Rossby waves are better able to transport momentum. The vorticity flux is thus stronger in the upper layer than the lower and, using (TL.3), the surface winds are positive (eastward) in the mid-latitude baroclinic zone (see Fig. 3.12).

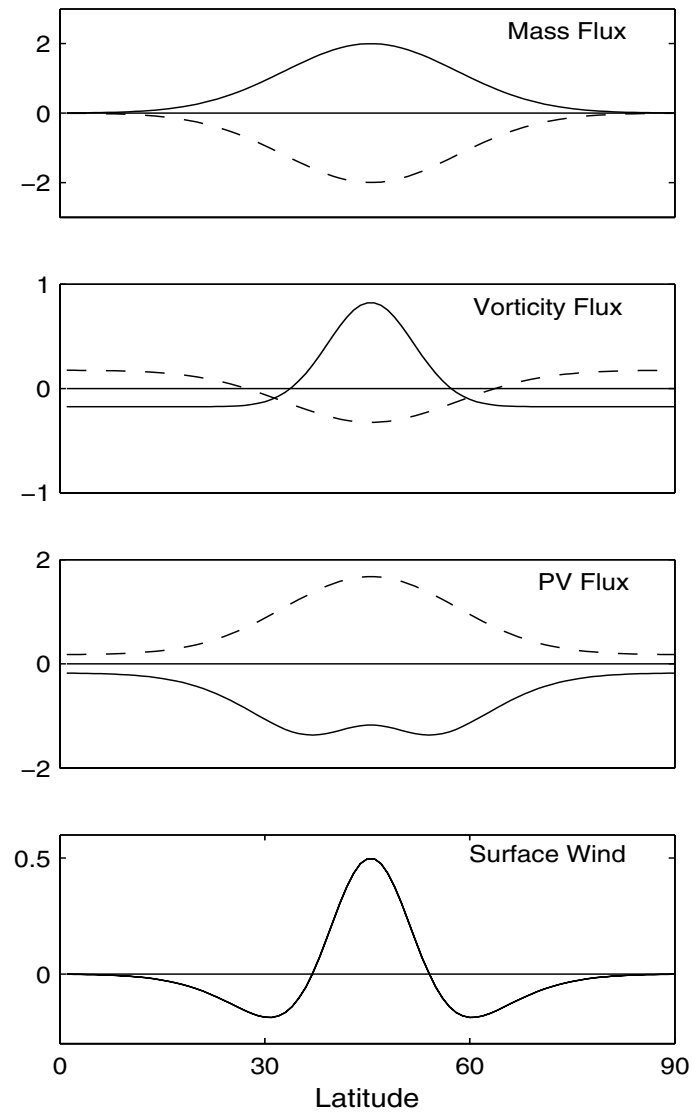


Fig. 3.12 Schema of the eddy fluxes in a two-layer model of an atmosphere with a single mid-latitude baroclinic zone. The upper layer fluxes are solid lines, the lower layer fluxes are dashed.

Momentum balance and the overturning circulation

In the upper layer the balance is between the vorticity flux and the Coriolis term, namely

$$f_0 \bar{v}_1 = -\overline{v'_1 \zeta'_1} < 0. \quad (3.85)$$

In lower layer

$$r \bar{u}_2 \approx f_0 \bar{v}_2 = -\frac{H_1}{H_2} f_0 \bar{v}_1 > 0. \quad (3.86a,b)$$

where the second inequality follows by mass conservation of the Eulerian flow.

In terms of the TEM form of the equations, (3.69), the corresponding balances in the center of the domain are:

$$f_0 \bar{v}_1^* = -\overline{v'_1 q'_1} > 0, \quad (3.87a)$$

and

$$r \bar{u}_2 = f_0 \bar{v}_2^* + \overline{v'_2 q'_2} = -f_0 \frac{H_1}{H_2} \bar{v}_1^* + \overline{v'_2 q'_2} = \frac{H_1}{H_2} \overline{v'_1 q'_1} + \overline{v'_2 q'_2} > 0, \quad (3.87b)$$

using mass conservation. An example of the dynamical balances of the two-layer model is given in Fig. 3.12)

3.7 THE ANTACTIC CIRCUMPOLAR CHANNEL

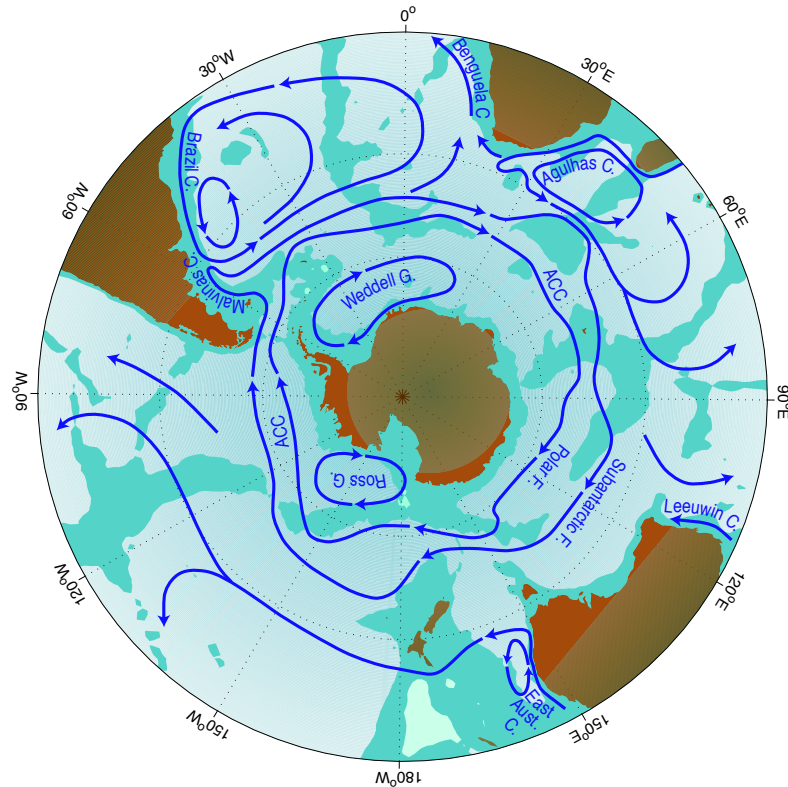


Fig. 3.13 Schema of the major currents in the Southern Ocean. Shown are the South Atlantic subtropical gyre, and the two main cores of the ACC, associated with the Polar front and the sub-Antarctic front.¹

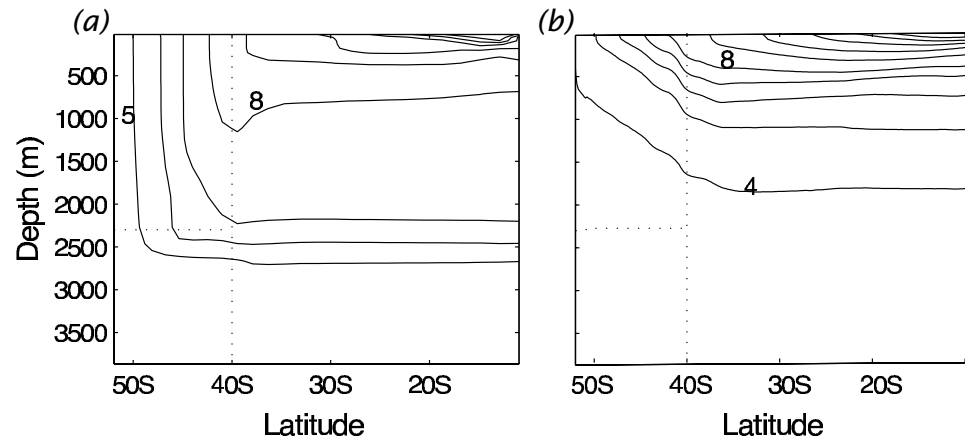


Fig. 3.14 The zonally-averaged temperature field in numerical solutions of the primitive equations in a domain similar to that of Fig. ?? (except that here the channel and sill are nestled against the polewards boundary). Panel (a) shows the steady solution of a diffusive model with no baroclinic eddies, and (b) shows the time-averaged solution in a higher resolution model that allows baroclinic eddies to develop. The dotted lines show the channel boundaries and the sill.²

3.7.1 Vertically integrated momentum balance

$$\mathbf{f} \times \mathbf{u} = -\nabla\phi + \frac{\partial \tilde{\boldsymbol{\tau}}}{\partial z}, \quad (3.88)$$

where $\tilde{\boldsymbol{\tau}}$ is the kinematic stress (and henceforth we drop the tilde). Integrating over depth

$$\mathbf{f} \times \hat{\mathbf{u}} = -\nabla\hat{\phi} - \phi_b \nabla\eta_b + \boldsymbol{\tau}_w - \boldsymbol{\tau}_f, \quad (3.89)$$

The x-component

$$f\hat{v} = -\frac{\partial \hat{\phi}}{\partial x} - \phi_b \frac{\partial \eta_b}{\partial x} + \tau_w^x - \tau_f^x, \quad (3.90)$$

Zonal average:

$$\oint [\phi_b \frac{\partial \eta_b}{\partial x} + \tau_w^x - \tau_f^x] dx = 0. \quad (3.91)$$

Form drag dominates at the bottom.

The vorticity balance - take curl of (3.89)

$$\beta\hat{v} = \mathbf{k} \cdot \nabla\phi_b \times \nabla\eta_b + \text{curl}_z \boldsymbol{\tau}_w - \text{curl}_z \boldsymbol{\tau}_f. \quad (3.92)$$

After zonal average $\beta v \approx 0$. Sverdrup balance cannot hold on average!

3.7.2 Form drag and baroclinic eddies

Form drag:

$$\tau_i = -\overline{\eta_i \frac{\partial p_i}{\partial x}} = -\rho_0 f \overline{\eta_i v_i} \quad (3.93)$$

Zonally-averaged meridional transport in each layer by

$$V_i = \int_{\eta_i}^{\eta_{i-1}} \rho_0 v \, dz \quad (3.94)$$

Momentum balance in fluid layers:

$$-f \overline{V}_1 = \tau_w - \tau_1 = \overline{\eta_1 \frac{\partial p_1}{\partial x}} + \tau_w, \quad (3.95a)$$

$$-f \overline{V}_i = \tau_{i-1}^x - \tau_i = -\overline{\eta_{i-1} \frac{\partial p_{i-1}}{\partial x}} + \overline{\eta_i \frac{\partial p_i}{\partial x}}, \quad (3.95b)$$

$$-f \overline{V}_N = \tau_{N-1} - \tau_N = -\overline{\eta_{N-1} \frac{\partial p_{N-1}}{\partial x}} + \overline{\eta_b \frac{\partial p_b}{\partial x}} - \tau_f, \quad (3.95c)$$

The vertically integrated meridional mass transport must vanish, and thus summing over all the layers (3.95) becomes

$$0 = \tau_w - \tau_f - \tau_N \quad (3.96)$$

or, noting that $\tau_N = -\overline{\eta_b \partial p_b / \partial x}$,

$$\boxed{\tau_w = \tau_f - \overline{\eta_b \frac{\partial p_b}{\partial x}}} \quad (3.97)$$

Momentum dynamics in height coordinates

$$-f_0 \bar{v}^* = \nabla_m \cdot \mathcal{F} + \frac{\partial \tau}{\partial z} \quad (3.98)$$

$$\nabla_m \cdot \mathcal{F} = -\frac{\partial}{\partial y} \overline{u'v'} + \frac{\partial}{\partial z} \left(\frac{f_0}{N^2} \overline{v'b'} \right) = \overline{v'q'}. \quad (3.99)$$

Potential vorticity flux scales as

$$\frac{\partial}{\partial y} \overline{u'v'} \sim \frac{v'^2}{L_e}, \quad \frac{\partial}{\partial z} \left(f_0 \frac{\overline{v'b'}}{b_z} \right) \sim \frac{v'^2}{L_d} \quad (3.100)$$

where L_e is the scale of the eddies and L_d is the deformation radius.

So that

$$-f_0 \bar{v}^* \approx \frac{\partial \tau}{\partial z} + \frac{\partial}{\partial z} \left(f_0 \frac{\overline{v'b'}}{b_z} \right). \quad (3.101)$$

and

$$\tau_w = \tau_f - \left[f_0 \frac{\overline{v'b'}}{b_z} \right]_{-H}^0, \quad (3.102)$$

Mass fluxes and thermodynamics

Eulerian

$$f_0 \bar{v}_a = \tau \quad (3.103)$$

TEM Thermodynamic:

$$\frac{\partial \bar{b}}{\partial t} + J(\psi^*, \bar{b}) = Q[b] \quad (3.104)$$

where $J(\psi^*, \bar{b}) = (\partial_y \psi^*)(\partial_z \bar{b}) - (\partial_z \psi^*)(\partial_y \bar{b}) = \bar{v}^* \partial_y \bar{b} + \bar{w}^* \partial_z \bar{b}$, ψ^* is the streamfunction of the residual flow and $Q[b]$ represents heating and cooling, which occurs mainly at the surface.

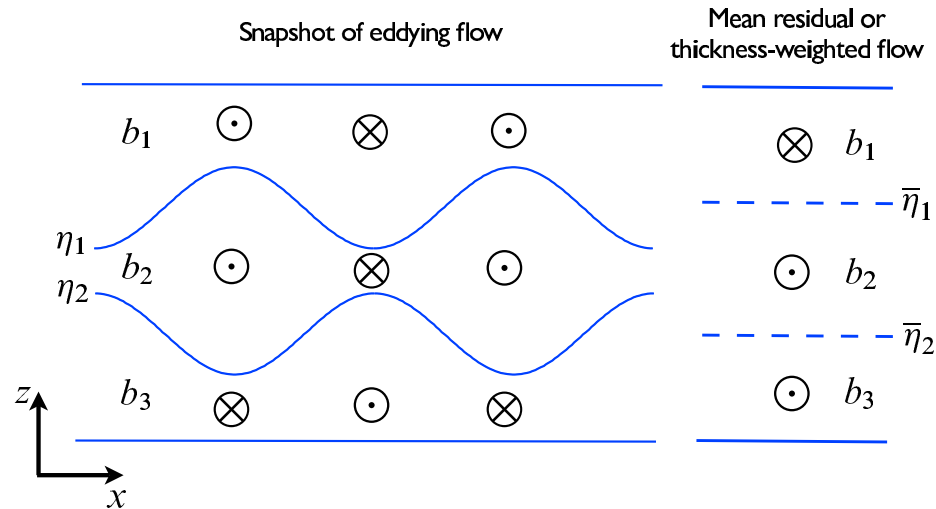


Fig. 3.16 A schema of the meridional flow in an eddying channel. The eddying flow may be organized (for example by baroclinic instability) such that, even though at any given level the Eulerian meridional flow may be small, there is a net flow in a given isopycnal layer. The residual (\bar{v}^*) and Eulerian (\bar{v}) flows are related by $\bar{v}^* = \bar{v} + \overline{v'h'/h}$; thus, the thickness-weighted average of the eddying flow on the left gives rise to the residual flow on the right, where $\bar{\eta}_i$ denotes the mean elevation of the isopycnal η_i .

Adiabatic:

$$J(\psi^*, \bar{b}) = 0, \tag{3.105}$$

Therefore $\psi^* = G(\bar{b})$

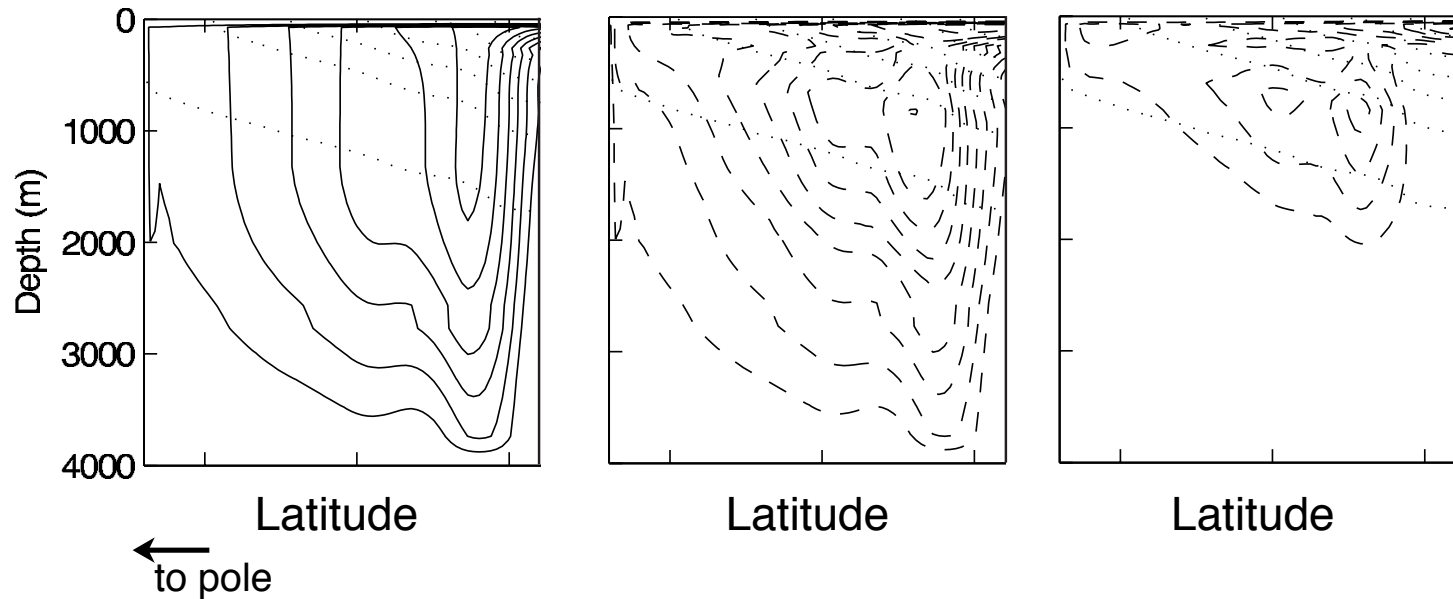


Fig. 3.17 The meridional circulation in the re-entrant channel of an idealized, eddying numerical model of the ACC (as in Fig. 3.14, but showing only the region south of 40°S). Left panel, the zonally averaged Eulerian circulation. Middle panel, the eddy induced circulation. Right panel, the residual circulation. Solid lines represent a clockwise circulation and dashed lines, anticlockwise. The faint dotted lines are the mean isopycnals. Over much of the channel the model ocean is losing buoyancy (heat) to the atmosphere and so the net, or residual, flow at the surface is polewards.